The Interaction of Mantle Plumes with Surface Thermal and Chemical Boundary Layers: Applications to Hotspots on Venus

Suzanne E. Smrekar
Jet Propulsion Laboratory
California Institute of Technology
MS 183-501
4800 Oak Grove Dr.
Pasadena, CA 91109

and

E. Marc Parmentier
Brown University
Department of Geological Sciences
Providence, RI 02912

submitted to Journal of Geophysical Research
October, 1994

Abstract

Large volcanic swells on Venus are believed to be a manifestation of mantle upwelling, or hotspots. The study of these regions provides important information on the interior of the planet. Numerical experiments arc carried out to examine the interaction of mantle plumes with the thermal lithosphere and a layer of depleted mantle, a product of pressure-release melting, using an axisymmetric finite element/finite difference code that incorporates temperature-dependent viscosity and pressure-release melting. The lithosphere is defined as a high viscosity lid; plumes arc initiated and maintained by a prescribed temperature at the base of the computational domain. The topographic uplift, geoid-to-topography ratio, and the volume of pressure-release melt are compared to estimated values for possible hotspots on Venus to constrain the properties of plumes and the lithosphere. The effects of lithospheric thickness, depleted layer viscosity and thickness, mantle temperature, and plume temperature and duration cm surface observable are predicted. Models with a thermal lithospheric thickness of approximately 100-150 km are consistent with observations, assuming a mantle temperature of 1300°C, a maximum plume temperature of approximate] y 1 S(K)°C, and mantle plume durations of 150-250" m. y. To be consistent with estimated volumes of volcanics at venusian hotspots, a significantly thinner thermal lithosphere requires a much cooler mantle; a thicker lithosphere requires a hotter mantle. Models with a depleted layer thickness of 100-250 km, in addition to a 1(K) km thick thermal lithosphere, predict the range of parameters found on Venus. Interpretation of large volcanic swells on Venus based on the evolutionary sequence predicted here implies that Beta, Atla, Western Eistla, and Imdr Regiones overlie either active or recently active mantle plumes. The geoid-to-topography ratio at Beta Regio is much larger than values found at other hotspots, and may indicate that it is in an early stage of evolution, or that the chemical or thermal boundary layers arc significantly thicker. Bell, Dione, and Themis Regiones appear to represent very late stage, possibly now extinct, hotspots. An estimate of the total plume buoyancy flux for Venus is much lower than the value obtained for Earth. The low buoyancy flux and small number of active plumes suggest a relatively low fraction

of bottom heating from the core. The small areal distribution of volcanism is consistent with a low level of ongoing resurfacing at a few active hotspots.

introduction

Hotspots, the surface manifestation of mantle upwelling, are characterized by broad topographic rises, volcanism, usually in the form of volcanic edifices, and extension. The amount of uplift and volcanism occurring at hotspots is strongly influenced by the properties of plumes, the lithosphere, and the upper mantle. Since mantle plumes arc difficult to observe using seismic techniques [*Nataf and VanDecar*, 1993] most information is obtained by studying their interaction with the lithosphere. Examination of the relationship between the gravity and topography at hotspots has revealed the importance influence of the low viscosity zone on Earth [*Richards and Hager*, 1984; *Robinson and Pm-sons,* 1988; *Richards et d.,* 1988; *Ceuleneer et al.*, 1988] and the probable absence of a similar region on Venus [*Phillips*, 1990; *Smrekar and Phillips, 1991; Kiefer and Hager*, 199 1]. The comparison of the properties of hotspots with models of mantle plume-lithosphere interaction also provide constraints on plume strength, buoyancy flux, and the role of lithospheric heating *[Davies,* 1988; *Liu and Chase,* 1989; *Sleep,* 1990; *Magna et al., 1993; Monnereau et al., 1993; Ribe and Christensen,* 1994].

Information about the lithosphere and mantle of Venus comes from studies of the gravity and topography, estimates of the effective elastic thickness, and a variety of indirect sources. Laboratory studies of dry diabase, the best analogy for the crust of Venus, show that the crust is likely to be very strong despite the surface temperature of 500°C, although weaker than olivine [*Mackwell et al.*, 1993]. Estimates of the effective elastic thickness from analyses of the topography [*Solomon and Head, 1990; Sandwell and Schubert, 1992; Johnson and Sandwell,* 1994] and the gravity and topography [*Phillips*, 1994; *Smrekar, 1994]* range from 1()-5() km.

Recent studies of Venus suggest that the structure of the lithosphere and heat flux out of the interior may be quite different than inferred prior to Magellan [*Solomon and Head, 1990].* Examination of the impact cratering record indicates that the average resurfacing age of Venus is between 200 and 6(K) my. [*Schaber et al., 1992; Phillips et al., 1992; Schaber et al., 1994],* a much older age than anticipated. The distribution of craters can not be distinguished from a

random distribution, implying that if resurfacing is ongoing, the dimension of areas being resurfaced is less than the average distance between craters, approximate] y 500 km *[Phillips et al., 1992].* The percentage of craters modified by either tectonism or volcanism is much lower than would be expected if the rate of resurfacing was constant in time and implies that the rate of resurfacing was much higher in the past and decreased abruptly [*Schaber et al.,* 1992; *Phillips et al., 1992].*

A variety of models have been proposed to explain the rapid change from high rates of tectonism and volcanism to apparently more modest present-day rates. In most models, a thick thermal lithosphere is responsible for the presently low rates of resurfacing. One hypothesis is that the decline in resurfacing rate could be accomplished by a decline in the strainrate caused by a secular decrease in mantle heat flux *[Solomon,* 1993]. Several studies have suggested that tectonics are episodic on Venus due to either chaotic convection [*Arkani-Hamed, 1993]* or to overturn of a thick, gravitational y unstable mantle upper boundary layer [*Parmentier and Hess, 1992; Turcotte, 1993].* The presence of a low density layer of residuum, a product of pressure-release melting, gives the surface boundary layer added positive chemical buoyancy and affects the time scale of overturn [*Parmentier and Hess,* 1992]. On Earth, much of this material is believed to be recycled back into the mantle by subducting plates. However, under stable continental interiors, a residuum layer may reach substantial thicknesses [e.g. *Jordan,* 1988]. Since Venus lacks vigorous mantle subduction, residuum may accumulate to thicknesses of several hundred kilometers [*Parmentier and Hess, 1992].*

Given that the impact crater distribution implies very low levels of resurfacing, hotspots may be one of the few tectonic settings of present day geologic activity. Detailed analysis of the gravity and topography data of Beta, Atla, and Western Eistla Regiones imply the presence of an active mantle plume at depth *[Grimm and Phillips,* 1992; *Phillips, 1994; Smrekar,* 1994]. At least six other regions may also be sites of mantle upwelling [*Stofan et al., 1994].* These regions of possible ongoing activity may offer important clues on present day resurfacing and the role of plume strength and the upper thermal and chemical boundary layers in controlling levels of tectonic

and volcanic activity. Although numerous regions have been identified as possible hotspots, at least one region, Bell Regio, appears to be in a very late stage of evolution, possibly extinct [*Smrekar,* 1994].

A primary goal of this study is to usc models of plume-lithosphere interactions, both with and without a near surface layer of depleted mantle, to provide constraints on the present-day thickness of the lithosphere and the existence of a possible layer of depleted mantle. We examine the effects of lithospheric thickness, depleted mantle layer thickness and viscosity, mantle temperature, and plume temperature and duration on the predicted evolution of topographic uplift, geoid-to-topography ratio, and estimated volumes of pressure-release melting. Another goal is to compare these predictions to observations of venusian volcanic swells to determine the evolutionary stage of hotspots and estimate their contribution to present day resurfacing and mantle heat flux. Below we describe the characteristics of possible hotspots cm Venus, the approach used to simulate mantle upwelling, model results, and discuss the implications for the properties of plumes and the lithosphere, hotspot evolution, and resurfacing on Venus.

Characteristics of Venusian Volcanic Rises

Magellan radar images, topography data, and gravity data have vastly increased our knowledge of the tectonic history and interior structure of hotspots on Venus. A variety of recent studies have examined the tectonics of the major volcanic rises on Venus, Beta, Atla, Bell, and Western Eistla Regio, using Magellan radar images *[Solomon et al.*, 1992; *Grimm and Phillips, 1992; Senske et al,* 1992; *Stofan et al., 1994]. Stofan et al. [1994]* have looked at these four primary hotspots as well as other regions of possible large scale mantle upwelling, including Imdr, Dione, Central Eistla, and Eastern Eistla Regiones. Their study divides possible upwelling locations into rift-dominated, volcano-dominated, and corona-dominated rises. They estimate the average diameter, height, and volume of the topographic swells, as well as the volume of any volcanic edifices, and the value of apparent depth of compensation for those regions where it had not been previously calculated. The swell heights are found by using topographic profiles to

estimate and remove the added height of any volcanic edifices. Swell heights are in the range of 1-2.5 km. Swell diameters are in the range of 12(X)-22(K) km (see *Stofan et al.* 1994 for estimation technique). The volume of edifices ranges from approximate] y 104 to 10^5 km^3. The study finds that the different morphologic classes of possible hotspots arc unlikely to represent different stages of hotspot evolution and that geologic relationships such as the timing of volcanism relative to extension or uplift is typically of little value for identifying evolutionary stage. However, the gravity, topography, and presence of volcanism can be used to identify the general stage of evolution in many cases.

The apparent depth of compensation for these regions varies from -1 (K) km, at Themis Regio, to 225-360 km at Beta Regio [*Herrick et al.,* 1989; *Smrekar and Phillips,* 1991; *Grimm and Philips,* 1992; *Smrekar, 1994; Stofan et al.,* 1994-]. In terms of GTR, this range cm-responds to approximate] y 15 to 35 m/km [*Smrekar and Phillips,* 199 1]. *Smrekar [1994]* looked in detail at the high resolution Magellan gravity data for Beta, Atla, Bell and Western Eistla Regiones. As concluded in several previous studies, Beta, Atla, and Western Eistla Regiones were interpreted as active mantle plumes [*Herrick et al., 1989; Smrekar and Phillips, 1991; Kiefer and Hager, 1991; Grim)?? and Phillips,* 1992]. Bell Regio, which was previously believed to be an active hotspot [*Smrekar and Phillips, 1991], was* interpreted as either inactive or in a very late stage of evolution based on the large effective elastic thickness, relatively shallow depth of compensation, and the small component of buoyancy force at the bottom of the lithosphere [*Smrekar, 1994].* Estimates of apparent depth of compensation or GTR can vary based on the method of analysis and especially on the wavelength range included in the study. Values that arc most useful for this study are those which filter out the shorter wavelength information that is typically related to volcanic edifices.

Model Description

The rise of a mantle plume and its interaction with the surface thermal and chemical boundary layers of mantle convection are studied using an axisymmetric finite difference scheme to describe the time evolution of temperature and chemistry variations. A standard penalty function

finite element formulation with linear rectangular elements is used to solve the buoyant, viscous flow equations. Advection terms in the energy (temperature) equation are approximated with an explicit, weighted-upwind differencing method. Nondiffusing chemical variation are calculated using a particle-in-cell t ypc method [cf. *Jha et al.*, 1994; and other studies cited therein]. Time steps arc limited by a Courant condition, which prevents fluid from moving farther than the dimension of one grid spacing over a time step. In general the resolution of the finite difference grid on which the temperature and chemical composition arc calculated can be different from the finite clement grid for the buoyant viscous flow. The results reported here usc a finite difference grid with twice the finite element resolution. Every other finite difference grid point coincides with a finite element node point. At each time step, velocities on the finite difference grid are calculated by linear interpolation from node point velocities on the coarser finite element grid. The rectangular grid has nonuniform spacing (Figure 1) to provide enhanced resolution in the plume and surface boundary layer.

Rather than being allowed to develop from an unstable thermal boundary layer, the plume in this study is prescribed as a hot region on the bottom of the domain with a maximum temperature at the symmetry axis. A gaussian radial temperature distribution typical of mantle plumes arising from an unstable thermal boundary [*Olsen et al., 1993]* is assumed. The width of the plume at the bottom of the domain is chosen to give a topographic uplift similar to hotspot diameters. In most experiments, the plume is turned off at a prescribed time after the start of the calculation by returning the hot region to the same temperature as the surrounding mantle. The vertical normal stress and shear stress are assumed to vanish on the bottom boundary so that upwelling in the plume is driven only by buoyancy forces within the model domain. This also allows upwelling flow through the bottom of the domain. Boundary conditions are rigid (vanishing horizontal and vertical velocity) at the top of the cylindrical region. Normal and shear stresses also vanish at the vertical outer boundary of the cylindrical domain.

Particular attention is given to the effects of melting, thermal structure, and viscosity in the plume and upper boundary layer. In addition to a thermal boundary layer, most models include a

layer of buoyant, depleted mantle at the surface. The initial temperature variation with depth is defined by an error function, with a constant initial temperature in the interior. The surface and interior temperatures are fixed at 500°C and 1300°C, respectively. The base of the lithosphere, as defined in this study, occurs at the depth where the temperature is 11 00°C. At temperatures below this value, the high viscosity allows very little horizontal flow.

The cylindrical computational domain has a height and radius of 24(K) km. This radius is significant y greater than the 600-1200 km radius typical of Venusian hotspots. If Venus has whole mantle convection, this height is roughly three quarters of the thickness of the convecting mantle. The finite clement mesh is 60 by 60 elements; the finite difference mesh has twice this resolution to ensure accurate estimation of the temperature and density changes due to melting. The resolution is the highest in the upper part of the mantle and lithosphere and along the axis where the plume rises. In the top and central 6(K) km the spacing is 1() km, grading into a spacing of 30 km in the rest of the region (Figure 1).

The layer of depleted mantle material extends from the surface to a depth below the base of the thermal lithosphere. The degree of melting is assumed to be 20% in the depleted region. This value is consistent with the amount of melting required to produce a basaltic crust, based on the amount of clinopyroxene and garnet in the source, and is the maximum value of melting allowed in our models. The density deviation from normal mantle material at 1300°C in each clement is $\Delta\rho = \rho_m\alpha(\Delta T - B\sigma)$ where pm is the mantle density, α is the coefficient of thermal expansion (3×10^{-5} C^{-1}), AT is the temperature difference between the mantle and the plume, B is a constant, and σ is the fraction of depletion. For B equal to 2500°C, the density contrast at 20% depletion is equivalent to that produced by a 500°C temperature anomaly. The chemical variation in density varies linearly from undepleted mantle (3300 kg/km^3) to 2950 kg/km^3 at 20% depletion.

The degree of melting in the mantle is calculated as $(T - T_m)/(L/c_p)$, where T is the temperature in an element, T_m is the melting temperature, L is the latent heat of fusion, and C_p is the specific heat. Wc usc a value of 600" kJ/kg [*Hess*, 1992] for the latent heat and 1 kJ/kg°C for the specific heat. The pressure-dependent solidus for dry peridotite [*Takahashi and Kushiro*,

1983] is represented by Tm = 11(K)+ 1.75 z, where z is the depth in km. The pressure-release melt is assumed to be extracted from the mantle and produce volcanism or crustal underplaying. This new volume of material is not directly included in the models. The effect of melt on the gravity and topography are considered separately.

The viscosity is based on a flow law for dry olivine. The viscosity function of the Arrhenius form is given by $\eta=\eta^*\exp(Q/RT)$ where Q is the activation enthalpy, R is the gas constant, T is the temperature and η^* is a theological constant. The activation enthalpy for dry olivine is 535 kJ/mole [*Chopra and Patterson, 1984]*. A value for η^* of ().12 gives a viscosity of 1021 Pas at a temperature of 1300°C. The viscosity is allowed to vary up to a factor of 1 (K) from the interior viscosity; larger viscosity variations are not accurately resolved and cause numerical instability. This viscosity range should be adequate to model the behavior of the plume and boundary layers. In some cases the viscosity is also a function of the degree of depletion. In these cases, the viscosity increases by a factor of 1() when the degree of depletion exceeds 2%. This increase in strength is based on the loss of water from the depicted material into the melt [*Karato et al., 1986]* and on the increased melting temperature of the residual mantle because of the larger Mg/Fe ratio [*Hess*, 1989].

The surface topography and gravity field for each model is calculated at chosen time intervals. The topography is found by balancing the calculated normal stress at the upper surface with the weight of the relief, ρgh, where p is density near the surface, taken to be the density of basalt, 29(K) kg/km^3, g is the acceleration of gravity, 8.87 m/s^2, and h is the surface topography. To take advantage of FFT methods, the surface topography and the variation in density due to both chemistry and temperature in each row of elements in axially symmetric geometry arc interpolated onto a three-dimensional Cartesian grid. The resulting contributions to the gravity field are calculated in the Fourier transform domain. We calculate the geoid-to-topography ratio, the least squares slope of the total geoid and topography, at an altitude of 300 km for comparison to values calculated over venusian hotspots.

The gravity and topography due to melt generation are treated separably. The volume of pressure-release melting can be a significant fraction of the total swell topography, but the distribution of the melt products is uncertain. The only information on the melt volume at venusian hotspots comes from estimates of volcanic edifice volumes. The relationship between the total volume of pressure-release melting and the volume of the edifices is difficult to estimate even on Earth. Based on seismic data interpretation, the volume of crust at thickening appears to be several times that of the volcanic edifices. Seismic data at a variety of oceanic terrestrial hotspots indicate that crustal thickening is confined to a region several hundred kilometers in radius [*White*, 1993, and references therein]. Underplating appears to be distributed over a slightly broader region. However, because of the difficulty of interpreting seismic profiles in the lower crust, estimates of the percentage of melt that is underplayed at Hawaii range from 15% [*Lindwall*, 1988] to 40% [*Watts et al.*, 1985; *ten Brink and Brother, 1987]*. Models of the seismic and gravity data at the Marquesas give estimates of the thickness of underplated melt of between 2 and 8 km [*Wolfe et al., 1994]*. Given the large uncertainty due to nonuniqueness in interpretation of both seismic and gravity data, an approximate estimate of the ratio of the volume of the volcanic edifice to the total melt volume is 1:2 to 1:10. Although there maybe differences in composition, temperature, crustal density, lithospheric thickness or other factors that would alter the ratio for venusian hotspots, this broad range is likely to be generally appropriate. Based on the range of volcanic edifice volumes for venusian hotspots of 104-105 km^3 [*Stofan et al.*, 1994] and the estimated edifice to total melt volume ratio, the total melt volume is likely to be 104-106 km^3. Below we consider the effects of two extreme cases, one in which all of the melt goes to form a volcanic edifice, and one in which 10% of the melt forms a volcano and 90% of the melt thickens the crust over a region 3(K) km in radius.

The plume temperature and velocity arc used to estimate plume buoyancy flux for comparison to terrestrial hotspots. on Earth, buoyancy flux can be estimated as Mgv, where M is the total mass per unit distance along the hotspot track, g is the acceleration of gravity, and v is the plate velocity [Davies, 1992]. M is found using the cross sectional area of the hotspot swell. On

Venus, where is there is no plate motion, this approach is not possible. In this study we compare the buoyancy flux from our models that agree with the observations from venusian hotspots to estimated values for oceanic hotspots. Buoyancy flux is estimated as Mvg, where M is the anomalous mass of the plume, v is the plume velocity, and g is the acceleration of gravity. M is defined as $\rho_m \alpha \Delta T$, where AT *is* the temperature anomaly in the plume relative to the mantle. Vertical velocity and temperature are found at a depth of 18(K) km below the surface, where the plume head is fully formed but does not yet sense the upper surface.

In addition to buoyancy flux, the buoyancy of the chemical and plume temperature anomalies arc compared to the equivalent buoyancy of the topography. The total buoyancy of the plume, B_T, is defined as $\delta M_T g/dt$, where δM_T is the difference in the mass anomaly of the plume between chosen time intervals, and&is the time interval. Similarly, the buoyancy duc to chemical density variations, B_C, is found from mass anomalies relative to the undisturbed outer edge of the computational domain. We also calculate the equivalent buoyancy of the predicted topography, $B_H = V\rho_l g/\delta t$, where V is the swell volume, p_l is the assumed density of the lithosphere (2900 kg/m^3). The comparison of these three types of buoyancy provides insight on the forces responsible for topographic uplift.

Model Results

Topographic uplift, geoid-to-topography ratio, and pressure-release melting are predicted as a function of time during the interaction of a plume with chemical and thermal lithospheres. A series of parameter studies that examine the effects of thermal lithospheric and depleted layer thickness, plume strength and duration, and mantle temperature, arc carried out in relation to a nominal case, which has a thermal lithospheric thickness of 1(K) km, a depleted mantle layer thickness of 150 km (i.e. it extends 50 km below the thermal lithosphere). The maximum plume temperature at the base of the computational region is 1750°C; the plume is turned off after 150 m. y. The viscosity is temperature-dependent, and varies relative to a value of 1021 Pas at the mantle temperature of 1300°C. The viscosity range is limited to 1019 to 10^{23} Pas.

The interaction of the plume with the chemical and thermal boundary layers is shown in Figure 1. Before the plume encounters the lithosphere, the plume head is approximately spherical (Figure la). The maximum temperature difference between the plume and the mantle decreases from 450°C at the base to approximately 200°C at the base of the lithosphere. The plume head spreads out into a mushroom shape as it approaches the base of the lithosphere (Figure 1 b), and begins to displace the deepest portion of the depleted layer. The thermal lithosphere is thinned more slowly, since it has a higher viscosity and is shielded from the plume by the depleted layer. A small component of downward velocity at the edges of the plume head causes the depicted layer and the cold lithosphere to pile up in a ring at the base of the lithosphere, just beyond the thermal limit of the plume head (Figure 1c). Thinning of the thermal lithosphere above the plume is also evident. Pressure-release melting at the base of the depleted layer creates a new region of low density depleted material. This new volume of depleted material is advected away as the plume head flows outward and does not affected continued melting at the center of the plume head (Figure 1 c). Since the depleted material is constantly being advected away and not recycled through the convecting region, the depletion (or, equivalently, melting) is never much greater than 1%. For higher melt volumes and degrees of melting, a pocket of depleted material develops at the top of the plume head. Once the plume is turned off, the plume tail eventually dies out and the plume head cools and spreads out further (Figure 1 d).

A topographic swell forms as the plume hits the base of the depleted layer and the thermal lithosphere (Figure 2) and broadens as the plume head spreads out. Approximately 500 m of dynamic topographic uplift occurs before the plume reaches the base of the depleted layer. The geoid is dominated by the gravity due to the topography and by the negative density anomaly caused by the hot plume (Figure 2). Thinning of the thermal lithosphere introduces a negative density anomaly since the relatively high density lithosphere is replaced by material from the hot plume. As the plume cools, the negative density anomaly decreases. Where the thermal lithosphere has thinned, the higher density undepleted mantle loads the surface and depresses the peak of the topographic swell to form a flatten dome or plateau (Figure 2). Thinning the depleted

layer has the opposite effect on the gravity and topography. Since the maximum temperature difference between the plume head near the surface and the mantle does not exceed 250°C in these calculations, undepleted mantle is always more dense than the depleted mantle layer. If the depleted layer is very thick and is thinned extensively, the positive contribution to the gravity from replacing depleted mantle with undepleted mantle can outweigh the negative contribution from the plume thermal anomaly. This situation will be discussed below.

The evolution of buoyancy and surface observables (GTR, maximum topography, and melt volume) for the nominal case are shown in Figure 3. The peak topography above the plume reaches a height of 0.5 km approximately 7S my. after the start of the calculation. The maximum topographic relief attained in this model is 1.25 km 10 my. after the plume is turned off, at approximatel y 160 my. After this time, the topography subsides s1ow1 y as the plume dies out and the lithosphere eventually begins to cool.

The GTR decreases throughout the evolution of the plume (Figure 3). The initial GTR is very large while the low density anomaly in the plume head is still deep in the mantle. Once the plume head has flattened out at the base of the lithosphere, the GTR decreases more slowly, reflecting the effects of heating and thinning the thermal and chemical boundary layers. Note that the GTR decreases by only ~6 m/km between 100 and 3(K) m. y.; changes in the topographic relief arc more pronounced (Figure 3). Thus the GTR for a hotspot remains fairly constant over a very large portion of its evolution.

Melting begins at approximately 120 my., or 40 my. after the plume encounters the lithosphere. The swell is over 1 km high when melting begins. The cumulative melt volume is approximatel y 1(14 km^3 (Figure 3), an order of magnitude less than the maximum volume of the topographic swell. The maximum degree of melting in this case is less than 2%.

A comparison of the chemical, topographic and thermal buoyancies illustrates some interesting aspects of plume-lithosphere interaction. (Figure 3). The topographic buoyancy increases rapidly initially duc to dynamic uplift, increases more slowly while the plume is heating the lithosphere, and decreases quickly once the plume begins to die out. Chemical buoyancy

becomes positive once the ring of low density material at the edge of the plume head starts to form; new residuum from pressure-release melting also contributes. The thermal buoyancy increases as long as the plume is active, and slowly decreases as the plume is turned off at depth and the plume head begins to cool. Since the plume buoyancy is calculated at a depth of 1800 km below the surface, it initially exceeds the topographic buoyancy and decays mm-e rapidly once the plume is turned off. For the nominal plume case, with a maximum plume temperature of 450°C, the buoyancy flux is 1.7 Mg/s while the plume is active.

The height of the plume penetration into the chemical and thermal boundary layers has a strong effect on the amount of melt produced, as well as on the topographic uplift and GTR. Cases with lithospheric thicknesses, L, of 50, 1(K), and 150 km and no layer of residuum present arc illustrated in Figure 4. The topographic uplift is similar for L = 1(K) and 150 km. GTR is slightly higher for L = 150 km than for L = 1(K) km, since the low density plume head is deeper, giving a larger positive geoid signal. No melt is produced when L = 150 km. There is almost a three order of magnitude difference(104 to 107 km^3) in the amount of melt generated between L = 50 and 1(K) km (Figure 4), and the degrees of melting arc 9% and 2%, respectively. Because of the depth dependence of the melting curve, a larger difference in surface observables and degree of melting occurs between the L = 50 and 100 km cases than between the L = 100 and 150 km cases. The topography is approximately ().75 km greater for L = 50 km than for L = 1(K), 150 km. The GTR for L = 50 km is at least 5 mgal/km smaller than for the other cases, due to the shallow plume head and the high topography (Figure 4).

The effects of varying the thickness of the depleted layer, D, arc not as straightforward as those due a change in thermal lithospheric thickness. In contrast to increasing L, increasing D allows the plume to produce less topographic uplift (Figure 5). The thicker the depleted layer, the less it is stabilized by the high viscosity thermal lithosphere and the more easily it is thinned. Replacing depleted mantle material with denser, undepleted mantle creates a negative buoyancy force that reduces the topography. Generally, the lower the topography, the greater the GTR (Figure 5). Although the topography is greater when no depleted layer is present, the GTR is very

similar for D = 0 and D = 150 km. This is surprising, since when the depleted layer is present, topography is less and the plume head is somewhat deeper; both effects increase the GTR. The cause of the lower than expected GTR for the D = 1 S() km case is the positive density anomaly due to the ring of depleted material replacing undepleted mantle at the edge of the plume head. The contribution to the buoyancy from this effect was seen in Figure 3. For the D = 250 km case, thinning of the low density depleted layer is so great that the topography actually becomes negative after the plume dies out. Since the plume can more easily penetrate the residuum layer than the thermal lithosphere, the effect of depleted layer thickness on the amount of melt volume is smaller than for similar variations in thermal lithospheric thickness. For D = (), 150, and 2(K) km, the cumulative melt volume is approximately 10^4 km^3 (Figure 5). With D = 250 km, the volume is only 10 km^3.

If the viscosity of residuum is increased by a factor of 10 due perhaps to the lower water content, the effect of the depleted layer becomes closer to that of the thermal lithosphere in some respect% Thinning of the depleted layer still causes a decrease in the maximum topography as D increases (Figure 6), but not as large a decrease as when no viscosity increase is assumed (Figure 5). For D = 150 km, the higher viscosity has little effect since the depleted layer is somewhat stabilized by the thermal lithosphere. GTR generally decreases with increasing D and decreasing topography (Figure 6). The D = 2(K) and 250 km cases have a similar GTR, due to different chemical buoyancy effects. When D is thicker, a larger ring of depleted material piles up at the edge of the plume head, creating a relatively low density region that decreases the geoid. The increased viscosity has a strong effect on plume penetration. The degree of melting is decreased relative to cases with no viscosity increase, with less than 1 % melting for D = 150 km. No melt is produced for D ≥ 200 km.

Next wc examine the effects of plume strength by looking first at plume temperature and then at plume duration. The volume of melt produced is very sensitive to plume temperature at the base of the lithosphere. A 100°C change in the maximum initial plume temperature results in only a difference of approximately 20°C in the near-surface, maximum plume temperature. Because of

the gaussian shape of the temperature distribution at the center of the axisymmetric computational, even a large change in maximum temperature has a relatively minor effect on the plume temperature averaged over the entire heated region, giving only a minor difference in buoyancy flux between the three cases. Thermal diffusion decreases large temperature differences as the plume rises through the mantle. The effect of varying the initial, maximum plume temperature by plus or minus 100°C on the maximum topography, GTR, and melt volume is illustrated in Figure 7. The resulting near-surface maximum plume temperature differences relative to the average mantle temperature of 1300°C are approximately 180°C, 200°C, and 220°C. Only minor differences are seen in the maximum topographic uplift and GTR (Figure 7). However, the volume of melt produced is extremely sensitive to plume temperature. No melt is produced when the maximum temperature difference between the plume and the mantle is 180°C. The cumulative volume of melt increases to 104 km^3 and 105 km^3 for a temperature difference of 200°C and 220°C, respectively (Figure 7).

Plume duration has a very significant influence on the surface observables and is difficult to constrain given the trade-off between plume duration and strength. In all of the cases illustrated above, the mantle upwelling is turned off at the base of the computational domain after 150 my. Cases with a continuously fed plume and D = (), 150, 2(X), and 250 km arc shown to times of 250 my. in Figure 8. Towards the end of this time, topographic uplift is continuing to increase by ~5m/m.y, GTR is decreasing by -0.05 m/km/my., and melt volume is increasing by -100-500 km^3/m.y. Assuming that these rates of change arc representative of the next 100 my. of the calculation, topography would increase by 500 m, GTR would decrease by 2 m/km, and melt volume would increase by 104 km^3. These cases illustrate the tradeoffs between plume duration and boundary layer thickness. For the case with a depleted layer thickness of 250 km, melting is predicted after 160 my. with a continuous plume but no melt formed if the plume is turned off after 150 my. (see Figure 5). The degree of melting is approximate] y 1 % greater for cases with a plume duration of 250 my. than for those with a plume duration of 150 my. The changes in

topography and GTR are also significant for a difference in plume duration of 100 my., but are not as pronounced as the difference in melt volume (compare Figures 5 and 8).

The overall effect of varying the mantle temperature is similar to varying the plume temperature. Models with mantle temperatures of 1200°C, 1300°C, and 1400°C were examined, using a lithospheric thickness of 100 km and an initial plume-mantle temperature difference of 450°C. Increasing the mantle temperature creates slightly more topography due to the added buoyancy resulting from greater melt production. However, the GTRs for the three cases are nearly identical. The higher topography produces a larger gravity anomaly, leaving the GTR essentially unchanged. For a mantle temperature of 1200°C, no melt is produced. For temperatures of 1300°C and 1400°C, the cumulative melt volumes are 2x106 and 2x104 km^3, and the degrees of melting are 2 and 8%, respectively. Higher mantle temperatures also cause melting to begin more rapidly. Cases with a depleted mantle layer were also run with different mantle temperatures. The results arc very similar to the cases described above. The only additional factor is that higher mantle temperature gives the depleted layer a lower viscosity, resulting in several hundred meters more topography and a GTR that is approximately 1 m/km less for a change in mantle temperature of 1 00°C.

In the cases discussed above the effect of melt volume on swell topography and gravity is treated separately. The volume of pressure-release melt can be a Significant portion of the total swell volume, and hot intruded material may contribute to topography through thermal expansion [*Phipps Morgan et al., 1994*]. Additionally, large volcanos can produce significant gravity anomalies, even at observation altitudes of approximately 300 km [e.g. *Phillips, 1994]*. As discussed above, the distribution of melt is uncertain, and but can have an important effect on the predicted gravity and topography. In the models presented here, the melt is generated within a region approximately 50-250 km from the center of the plume (Figure 9). The greater the volume of melt produced, the larger the region of melting. In models of terrestrial plumes, *Farnetani and Richards [1994]* find that melt occurs over a region with a radius of 360-580 km. The variation in melt region size between the two studies is primarily due to the uniform temperature distribution in

the interior of the plume head used by *Farnetani and Richards* [1994] versus the gaussian temperature distribution used here. In models of pressure-release melting under Hawaii, *Watson and McKenzie [1991]* found that melting was concentrated in a region 40 km in radius. These models do not treat melt migration. The two end member possibilities are that melt migrates only vertically, or that melt is evenly distributed over the swell volume. As will be shown next, a very broad distribution of melt has little effect on the gravity and topography. For this reason, we concentrate on the case in which melt is confined to within 300 km of the axis. This fairly narrow distribution is also consistent with the distribution of crustal thickening and underplaying found for terrestrial hotspots, as discussed above.

To determine the effects of melt volume on the predicted gravity and topography, we assume an extrusive-to-intrusive ratio of 1:10. The extrusive volcanism forms a volcano at the surface and the intrusive volcanism is distributed as a layer of uniform thickness 300 km in radius within the crust. A model with an initial plume temperature of 550°C (see Figure 7) is used as an example since it predicts a melt volume of 105 km^3. This value lies in the middle of the estimated range of melt volume for venusian hotspots, based on volcanic edifice volume estimates of 104-105 km^3 [*Stofan et al.*, 1994] and assuming an extrusive-to-intrusive ratio of between 1:1 and 1:10. If 90% of the melt is assumed to be intrusive volcanism and is crustally compensated, it produces only tens of meters of topography and has very little effect on the gravity. Even if the volume of intrusive volcanism is great enough to produce several hundreds of meters of crustally compensated topography, the overall effect on the gravity and topography is minor.

For extrusive volcanism, the volcano produced is assumed to have a slope of 0.5°, which results in a maximum height of almost 2.5 km and a radius of approximately 300 km for this example. This size is typical of volcanic edifices located on topographic swells on Venus [*Stofan et al., 1994]*. If this size volcano is crustally compensated at a depth of 10 km (probably a minimum depth), the GTR decreases by as much as 2 m/km relative to the case when the effects of volcanism are ignored (Figure 10). Even though the topography of the volcano increases the gravity, the shallow crustal compensation acts to lower the total gravity. If a volcano of the same

size is uncompensated, or flexurally compensated, the contribution of the volcano topography to the gravity increases the GTR by up to 5 m/km (Figure 10). At least some volcanos on Venus may be largely flexurally compensated, as shown by detailed analysis of the gravity and topography at Bell and Atla Regiones [*Smrekar*, 1994; *Phillips*, 1994]. A much larger volcano would cause a significantly greater increase or decrease in the GTR, depending on the degree of isostatic compensation. The potential contribution of volcanos to the GTR underscores the importance of separating the swell and volcano portions of the gravity and topography when comparing data to models of swell formation.

Discussion

In this section, model results are compared with data on topography, GTR, and volcanic volumes for possible venusian hotspots to determine constraints that can be placed on the thickness of the boundary layers, mantle temperature, and plume strength. We also discuss the implications of model results for determining the evolutionary stage of individual hotspots. We then examine the role of hotspots, plume, and lithospheric properties in resurfacing history of Venus. Finally, venusian hotspots arc compared to terrestrial hotspots.

Observational Constraints on Lithospheric Properties

The thickness of the thermal lithosphere has a strong effect on predicted topographic uplift, GTR, and melt volume. For a plume duration of 150 my. or more, the amount of topographic uplift produced for a 50 km thick lithosphere is at the upper end of the observed volcanic swell heights of 1-2.5 km (Figure 4). For a mantle temperature of 1300°C and a maximum initial plume temperature of 1750°C, the volume of melt produced, almost 107 km^3, is much larger than the expected range of 1(14-106 km^3. A lithospheric thickness of 50 km would require a lower plume or mantle temperature to be consistent with observations. However, such a small lithospheric thickness is difficult to reconcile with large estimates of effective elastic thickness of 30-50 km at

hotspots [*Phillips*, 1994; *Smrekar*, 1994]. Thus the lower bound on thermal lithospheric thickness probably lies between 50 and 100 km. The lower bound is probably c1osc to 1(K) km, as the volume of melt produced with a combined plume and mantle temperature of 1500°C (initial temperature of 1750°C, see Figure 4), 10^3 km^3, is lower than typical volcanic edifice volumes. Holding other parameters the same, no melt is produced for a lithospheric thickness of 150 km. However, as noted above, a small change in the maximum plume temperature can have a very large effect on the volume of melt (see Figure 7). A higher plume or mantle temperature, or a longer duration plume, could produce volcanism without having a large effect on the topography or GTR, predicting allowable surface observables for a thermal lithospheric thickness in excess of 150 km. Although the upper bound on lithospheric thickness was not fully examined in this study, the importance of the pressure dependence of the melting temperature suggests that fairly extreme plume or mantle temperatures would be required to produce sufficient melt volumes for a lithosphere thicker than 200 km.

The possible range of depleted layer thickness was examined assuming a thermal lithospheric thickness of 100 km. The upper bound on the thickness of the depleted layer is constrained by the amount of thinning of the layer. Too large a thickness of depleted material leads to excessive thinning, very large GTRs, and little topographic uplift. For a plume duration of 150 to 250 m. y., 200 km is an upper bound on the thickness of the depleted layer. Even a much longer lived plume is unlikely to be able to produce sufficient topographic relief to be consistent with observations. Given a 1(K) km thick thermal lithosphere, a lower bound on the thickness of a depleted layer was not obtained. If the viscosity of depleted mantle is ten times that of undepleted mantle the upper bound on the depleted layer thickness is still close to 200 km.

Observational Constraints on Plume Strength and Mantle Temperature

The total plume strength is constrained by the height and diameter of the topographic swell and the volume of volcanics. However, the effects of mantle temperature, the temperature difference between the plume and mantle, and the duration of the plume can not be determined

independently. Most of the models shown above predict reasonable swell diameters and heights. A smaller number cases give an acceptable range of melt volume ($1\ 0^4$-10^6 km^3), which is also a function of lithospheric thickness. The constraints discussed above imply that the thermal lithosphere has to be approximately 100 km or more in thickness. Melt volume is less sensitive to depleted layer thickness since a plume can mm-c easily thin the low viscosity depleted layer. Accepting this bound on thermal lithospheric thickness, the melt volume is most sensitive to the maximum plume temperature.

For Venus, an additional unknown factor is the duration of the plume. The longer the plume lasts, the more it thins the lithosphere, and the higher it rises, producing significantly greater volumes of melt. Note that in these models the plume dots not reach the surface and cause uplift of several hundred meters until 60-75 m. y. after it begins to rise from a depth of 2400 km. Thus for cases with a duration of 150-250 my. the period of interaction of the plume with the surface is approximately 75-175 my. Although the duration of mantle plumes on Earth is not well constrained, for comparison the time span of the still active Hawaiian-Emperor hotspot is (thus far) -80 my. If flood basalts coincide with the initial location of a plume head, there is evidence of much longer duration plumes. The Karoo flood basalts began erupting approximately 200 Ma and appear to be linked to the Crozet hotspot [White *and McKenzie,* 1989]. Given a 1(K) km thick lithosphere and a plume duration of 150 my. (75 my. at the surface), the maximum plume temperature near the base of the lithosphere is restricted to -1500°C or more. If the plume lasts longer than 150 my., the maximum plume temperature could be lower than 1500°C. If the lithosphere is thicker than 100 km, the maximum allowable plume temperature is higher.

Implications for Interpretation of Hotspot Evolution

The earliest stage of hotspot evolution is characterized by very large GTR, low topography, and no volcanism. Using the present Magellan gravity data set, GTRs in excess of 40 mgals are not observed on Venus [*Simons et al., 1994].* However, high resolution gravity data is still being collected and processed for some high latitude hotspot candidates. If no regions with very large

GTRs occur on Venus, it may mean that there are no plumes in the very early stage of evolution. It is also possible that the earliest stage of evolution is difficult to observe both because it is likely to last for only a period of a few tens of millions of years (a much shorter period than intermediate and late stages) and because before the plume reaches the base of the lithosphere the topography is so low that the GTR might be difficult to calculate accurately.

The next stage of hotspot evolution is characterized by an active plume, a large GTR, significant topographic relief, and pressure-rchmse melting. The next stage occurs when the plume begins to die out but there is still a large thermal anomaly at depth. Pressure-release melting ceases once the plume stops rising. Surface topography and GTR decrease very slowly as the plume and lithosphere cool. In the final stage of evolution, the thermal anomaly is gone, causing both topography and GTR to become small. Possible examples of venusian hotspots in these intermediate and late stages of evolution are discussed next,

Beta, Atla, Western Eistla, and Bell Regiones appear to represent a range of evolutionary stage. Three of these regions are interpreted to be active. The GTR for Beta is 31 m/km, while Western Eistla and Atla have smaller values of 20 and 21 m/km, respectively [*Smrekar and Phillips, 1991]*. The heights of the swells at Beta, Western Eistla, and Atla are 2.1, 1.8, and 2.5 km, respectively [*Stofan et al.,* 1994]. Since the volume of pressure-release melting is a strong function of mantle and plume temperature, it can not be used to distinguish between intermediate and late stages. Both the high relief and the large GTRs at Beta, Atla, and Western Eistla Regiones imply active plumes in an intermediate stage of evolution. Detailed modeling of the gravity data at Atla Regio shows evidence of loading from below on the scale of the topographic swell, which was interpreted to indicate the presence of a thermal anomaly at depth [*Smrekar*, 1994]. As shown by the model results above, it is possible that the 10 m/km difference in GTR between Beta Regio and Western Eistla and Atla Regiones is a result of differences in the lithospheric structure. Specifically, a thick depleted layer or thermal lithosphere under Beta Regio could be responsible for the very large GTR. Although smaller in diameter, Imdr Regio has a large compensation depth and rise height of 1.6 km [*Stofan et al.*, 1994], and may be in a comparable evolutionary stage.

On the basis of low relief, small apparent depth of compensation, and evidence for a relatively minor contribution from bottom loading to swell topography, Bell Regio was interpreted to be in a very late stage of evolution, possibly extinct [*Smrekar*, 1994]. Themis and Dione Regiones are similar to Bell Regio in that they have fairly shallow compensation depths and relative] y low relief [*Stofan et* al., 1994], and may also represent very late stage hotspots. Overall, the evidence suggests numerous intermediate or late stage hotspots and few, if any early stage hotspots.

Rifting has been suggested as part of a predictable sequence of hotspot evolution. Some numerical and laboratory studies imply that rifting should proceed volcanism, since considerable topographic uplift usually occurs prior to any pressure-release melting [*Olsen and Nam*, 1986; *Griffiths and Campbell, 1991]*. Significant topographic uplift prior to pressure-release melting is also predicted in this study. However, geologic studies of terrestrial hotspots suggest that the timing of volcanism with respect to rifting varies [*Hooper*, 1990; *Hill,* 1991]. The key variable may be lithospheric temperature and thus strength [*Houseman and England, 1986; Hill, 1991].* If the lithosphere is already weak, rifting may occur rapidly. A colder lithosphere may not extend until it is heated by the plume, possibly after the start of volcanism. Additionally, the study of the morphology of hotspots by *Stofan et al. [1994]* found that extension and volcanism often overlap at venusian hotspots and that the relative timing of the two processes does not help to constrain the evolutionary stage. The absence of topographic swells that have only rifting without volcanism supports the hypothesis that the lithosphere is fairly thick and cold.

In addition to the broad topographic swells discussed above, the other major highland features found on Venus arc large, highl y deformed plateaus [e.g. *Bindschadler et al.*, 1992]. *Herrick and Phillips [1990]* and *Phillips et al. [1991]* have proposed that these plateaus are also mantle upwellings. In these models, the plateaus form though the production of large amounts of pressure-release melting and flood volcanism. Evidence for numerous episodes of deformation, embayment by surrounding plains volcanism [*Senske et al.*, 1994] and a somewhat higher crater density have been used to argue that venusian plateaus are amongst the oldest landforms on Venus

[*Ivanov and Basilevsky, 1993]*. If plateaus are very old and formed through the accumulation of huge volumes of pressure-releaw melting, the implication is that mantle or plume temperatures were much higher or that the lithosphere was much thinner than at present.

Comparisons to Terrestrial Hotspots

There are approximately 30 known hotspots on Earth [e.g. *Davies,* 1988; *Sleep, 1990, and refs. therein]*. They arc primarily located on oceanic plates, where the effect of lithospheric thickness on topography and gravity is clearly evident. As the lithosphere cools and thickens with age, the topography decreases and the GTR increases [*Cazenave et al.,* 1988]. In addition, the low viscosity zone thins at the expense of the thickening lithosphere. The presence of a significant low viscosity zone acts to decouple the topography from the buoyancy forces in the plume, resulting in lower topography and GTRs [**Robinson** *and Parsons,* 1988]. A comparison of GTRs for oceanic hotspots and venusian hotspots shows that GTRs for Venus area factor of 2-4 higher, which can bc interpreted to indicate that there is no low viscosity zone on Venus [*Smrekar and Phillips,* 199 *1]*. Since gravity data is more difficult to obtain, the relationship between gravity and topography is not well studied at most continental hotspots. In those regions where adequate data is available, continental hotspots were found to have slightly more shallow compensation depths (or, equivalently, slightly smaller GTRs) than typical oceanic hotspots [*Waschbusch and McNutt, 1994* and references therein]. In general, the effective elastic thicknesses at venusian hotspots arc comparable to those found for terrestrial hots pots, but compensation depths are typically larger.

The diameter, height, and volcanic edifice volume of venusian hotspots lies within the range found on Earth [*Stofan et al., 1994]*. On Earth, the buoyant y flux of hotspots is calculated by using plate velocity to integrate the swell volume over time [*Davies,* 1988; *Sleep, 1990]*. In the absence of a plate velocity, one must use a model to predict the minimum buoyancy flux required to maintain the hotspot swell. The buoyancy flux of most models in this study, which produces a swell with dimensions typical of Venusian hotspots is 1.7 Mg/s. This value is in the middle of the range of the buoyancy flux estimated for terrestrial plumes, 0.3 to -7 Mg/s [*Davies, 1988; Sleep,*

1990]. A common perception is that hotspots on Venus are larger than those on Earth. This may be a misconception due to the absence of plate motions on Venus. Additionally, if chemical buoyancy plays an important role in supporting terrestrial hotspots, thermal buoyancy flux for terrestrial hotspots may be overestimated.

Simple estimates of the buoyancy flux at hotspots is much less on Venus than on Earth. Even if there are ten active hotspots on Venus, which is certainly an upper bound, each with the value of buoyancy flux suggested by model results of 1.7 Mg/s, the total of 17 Mg/s is still only a fraction of the 56 Mg/s estimated for Earth. Fewer plumes on Venus is consistent with a greater portion of internal heating relative to bottom heating of the mantle. The contribution of hotspots to Earth's total heat flux is estimated to be 1()% *[Davies, 1988],* with mantle upwelling at ridges accounting for the other 90%. Other contributions to heat transfer are difficult to estimate on Venus. On Venus there is no system of spreading ridges, but volcanism is wide spread and smaller scale regions of mantle upwelling, in the form of corona, may also contribute to mantle heat loss [*Stofan et al.*, 1992].

Although it is tempting to interpret this results as an indication of a much smaller total heat flux on Venus compared to Earth, part of the difference in the pattern of heat loss maybe duc to a difference in heat source distribution. A large fraction of bottom heating predicts a small number of strong plumes that develop at the core-mantle boundary, and a large fraction of internal heating predicts numerous small upwellings that develop within the mantle with fewer, weaker plumes from the core-mantle boundary [*Bercovici et al.*, 1989]. The small number of major hotspots on Venus suggests a lesser proportion of internal heating on Venus relative to Earth. Additionally, mantle convection is a time-dependent phenomenon. Just as there have been past periods of greater and lesser plume activity on Earth [*Larson*, 1991], Venus is likely to have experienced considerable variability.

Implications for the Resurfacing History of Venus

Four hotspots, Atla, Beta, Imdr, and Western Eistla Regiones, have been interpreted as active. The presence of these four active hotspots is consistent with models of impact cratering history that allow for minor on going resurfacing [*Schaber et al.*, 1992; *Phillips et al., 1992]*. Certainly the area resurfaced by volcanic edifices associated with these hotspots is minor.

The general bounds on both thermal and chemical boundary layer thickness determined in this study are consistent with several models that relate thermal evolution of the planet to resurfacing history, such as episodic overturn of a thermal boundary layer along with a layer of depleted mantle [*Parmentier and Hess*, *1992]* and steady secular decline in heat flow *[Solomon,* 1993; *Grimm*, ***1994].*** Unless a plume is very long lived (> 300 my.), or the plume temperature exceeds 1600°C, the results of this study are inconsistent with models which predict thermal lithospheric thicknesses in excess of 150-200 km. Models that call for a very thick thermal lithosphere include episodic overturn of a solely thermal boundary layer [*Turcotte*, 1993] and varying heat flow duc to chaotic mantle convection [*Arkani-Hamed*, *1993]*.

Conclusions

Comparison of model predictions and estimates of GTR, topographic uplift, and volumes of volcanic edifices provide important constraints on the strength of mantle plumes and on the structure of the lithosphere. A thermal lithosphere of approximately 100 km is consistent with observations. A thinner lithosphere gives too much uplift, too low a GTR and too much volcanism. A significantly thicker lithosphere, of 150 km or more, could only produce sufficient pressure-release melting if the mantle plume is very long lived (> 300 my.) or if the mantle temperature is significantly hotter than 1300°C.

In many ways the effects of the interaction of a mantle plume with a layer of depleted mantle arc opposite to those of the interaction of a mantle plume with the thermal lithosphere because of the opposite sign of the resulting density anomal y. Given a thermal lithosphere of 100 km, the surface observable are consistent with a layer of depleted material in the range of 100-200”

km. A thicker depleted layer thins rapidly, creating a positive density anomaly when replaced by more dense undepleted mantle and decreasing the surface topography. For the range of plume temperatures considered and a depicted layer viscosity between one and ten times greater than that of undepleted mantle, the layer may be up to approximately 250 km in thickness. No pressure-release melting occurs if the depleted layer is 250 km or more in thickness for a mantle temperature of 1300"C.

Lack of constraints on the duration of plumes on Venus adds some uncertainty to bounds on plume properties. For the purposes of discussion, wc assume a duration of 150-250 my., which corresponds to a plume-lithosphere interaction period of approximate] y 75-175 my. Given a total plume duration of 150 m. y., a maximum plume temperature of 1500°C predicts melt volumes that are within an order of magnitude of the volume of volcanic edifices at individual plumes. There is considerable uncertainty in the relationship between volume of volcanic edifices and the total melt volume, but, based on analogy to terrestrial hotspots, the total melt volume is likely to be within an order of magnitude of the edifice volume. The models in this study assume a mantle temperature of 1300°C, giving a near surface plume-mantle temperature difference of 200°C. These values are comparable to those inferred for Earth [*Sleep*, 1990; *Watson and McKenzie, 1991; Nataf and VanDecar, 1993]*. Higher and lower combinations of mantle and plume temperatures will also fit the observations if the duration of the plume is adjusted. If the lithosphere is thicker than 100 km, a higher plume temperature is allowable.

The morphology of venusian hotspots is far more variable than terrestrial hotspots, and may reflect variations in the properties of the lithosphere or plume [*Stofan et al.,* 1994]. Despite this variety of hotspot features it is generally possible to determine the stage of evolution. The models presented here predict the evolution of topography, GTR, and melt production as the plume encounters the lithosphere, spreads, and eventually dies out. Although lithospheric thickness, depleted layer viscosity and thickness, and plume strength all affect the magnitude and timing of uplift, volcanism, and GTR, the same basic sequence always occurs for models that are consistent with observed hotspot parameters. The GTR dccrcascs rapidly while the plume is still deep in the

mantle, and more slowly once it encounters the lithosphere. The initial decrease is a result of the increasing contribution of the negative thermal density anomaly as it approaches the surface. Further decreases in the GTR are due to spreading of the plume head and thermal erosion of the lithosphere. Since GTR decreases monotonically over the lifetime of a plume, it provides the best indication of the evolutionary stage of the plume.

Interpretation of large volcanic swells on Venus based on the evolutionary sequence predicted here implies that Beta, Atla, Western Eistla, and Imdr Regiones overlie active mantle plumes. The GTR at Beta Regio is significantly larger than at other hotspots, indicating either an earlier stage of evolution or a thicker thermal lithosphere or depleted mantle layer. A difference in the properties of the lithosphere would be consistent with the interpretation that a block of cold, highly deformed lithosphere was present at Beta prior to the arrival of a mantle plume [*Senske et* al., 1992]. The relatively low values of GTR and swell height at Bell, Dione, and Themis Regiones arc interpreted to indicate very late stage, possibly extinct, hotspots. The overall heat flux from venusian hotspots is estimated to be a fraction of that from terrestrial hotspots. The smaller number of major hotspots on Venus as compared to Earth suggests a smaller fraction of internal heating.

An interesting observation is that there appear to be man y intermediate or late stage hotspots but no obvious young hotspots. Specifically, them are no topographic swells with large GTRs but no volcanism. This observation can be interpreted in several different ways. One argument is that given the small number of hotspots on Venus, and the fairly short duration of the early, high GTR, stage of hotspot evolution, one might not expect to observe an early stage hotspot. Alternatively, a high mantle or plume temperature would result in pressure-release melting very soon after initial uplift.

The few active hotspots and the relatively small area of the associated volcanic edifices are consistent with minor ongoing resurfacing. The results of this study alone cannot be used to distinguish between various models proposed to explain the resurfacing history of Venus. However, constraints obtained in this study show that the thermal lithosphere is approximately

l(K)- 150 km thick, given mantle plume and temperatures comparable to those estimated for Earth. Thus models that include a thermal lithospheric thickness in the range of approximately 100-150 km arc favored over models with a thicker lithosphere, unless the plume/mantle temperature is much higher on Venus than on Earth. These results further show that the relationship between gravity and topography at hotspots is not a simple function of the thermal lithospheric thickness, and that a variety of factors such as a chemical boundary layer, the effects of pressure-release melting, plume strength, and the stage of hotspot evolution all have a significant effect on the gravity and topography.

ACKNOWLEDGMENTS

This work was supported by NASA grant 889-62-02 to S.E.S. The research conducted by S.E.S. and presented in this paper was carried out at the Jet Propulsion Laboratory, California Institute of Technology, under a contract with the National Aeronautics and Space Administration. The JPL/Caltech Cray Supercomputer used in this investigation was provided by funding from the NASA Offices of Mission to Planet Earth, Aeronautics, and Space Science.

References

Arkani-Hamed, J., On the tectonics of Venus, *Phys. Earth Planet. Int., 76,75-96, 1993.*

Bercovici, D., G. Schubert, and G.A. Glatzmaier, Influence of heating mode on three-dimensional mantle convection, *Geophys. Res. Lett., 16,617-620, 1989.*

Bindschadler, D. L., G. Schubert, and W. M. Kaula, Coldspots and hotspots: Global tectonics and mantle dynamics of Venus, *J. Geophys. Res., 97, 13,495-13,532, 1992.*

Cazenave, A., K. Dominh, M. Rabinowicz, and G. Ceuleneer, Geoid and depth anomalies over ocean swells and troughs: Evidence of an increasing trend of the geoid to depth ratio with age of the plate, *J. Geophys. Res.,* 93, 8064-8077, 1988.

Ceuleneer, G., M. Rabinowicz, M. Monnereau, A. Cazenave, and C. Rosemberg, Viscosity and thickness of the sub-lithospheric low-viscosity zone: Constraints from geoid and depth over oceanic swells, *Earth Planet. Sci. Lett., 89,84-102, 1988.*

Chopra, P.N., and M.S. Paterson, The role of water in the deformation of dunite, *J. Geophys. Res.,* 89, 7861-7876, 1984.

Davies, G. F., Ocean bathymetry and mantle convection 1. Large-scale flow and hotspots, *J. Geophys. Res.,* 89, 10,467-10,480, 1988.

Davies, G. F., Temporal variation of the Hawaiian plume flux, *Earth Planet. Sci. Lett., 277-286, 1992.*

Farnetani, C. G., and M.A. Richards, Numerical investigations of the mantle plume initiation model for flood basalt events, *J. Geophys. Res.,* 99, 13,813-13,833, 1994.

Grimm, R. E., and R.J. Phillips, Anatomy of a venusian hot spot: geology, gravity and mantle dynamics of Eistla Regio, *J. Geophys. Res,* 97, 16,035-16,054, 1992.

Grimm, R. E., Recent deformation rates on Venus, *J. Geophys. Res.*, in press, 1994.

Griffiths, R.W., and I.H. Campbell, interaction of mantle plume heads with the Earth's surface and onset of small-scale convection, *J. Geophys. Res.,* 96, 18,295-18,31(), 1991.

Hess, P. C., *Origins of Igneous Rocks*, Harvard University Press, Cambridge, MA, 336 p., 1989.

Hess, P. C., Phase equilibria constraints on the origin of ocean floor basalts, in *Mantle Flow and Melt Generation at Mid-Ocean Ridges,* eds. J. Phipps Morgan, D.K. Blackman, and J.M. Sinton, Am. Geophys. Un. Geophys. Mono. 71,67-102, 1992.

Herrick, R. R., B. G. Bills, and S. A. Hall, Variations in effective compensation depth across Aphrodite Terra, Venus, *Geophys. Res. Lett., 16, 543-546, 1989.*

Herrick, R. R., and R.J. Phillips, Blob tectonics: A prediction for western Aphrodite Terra, Venus, *Geophys. Res. Lett., 17, 2129-2132,* 1990.

Hill, R.]., Starting plumes and continental break-up, *Earth Planet. Sci. Lett., 104,398-416, 1991.*

Hooper, P. R., The timing of crustal extension and the eruption of continental flood basalts, *Nature,* 345,246-249, 1990.

Houseman, G., and P. England, A dynamical model of lithospheric extension and sedimentary basin formation, *J. Geophys. Res., 91, 719-729,* 1986.

Ivanov, M. A., and A.T. Basilevsky, Density and morphology of impact craters on tessera terrain, Venus, *Geophys. Res. Lett., 20, 2579-2582, 1993.*

Jha, K., E.M. Parmentier, and J. Phipps Morgan, The role of mantle-depletion and melt-retention buoyancy in spreading center segmentation, *Earth Planet. Sci. Lett. 125, 221-234, 1994.*

Johnson, C. L., and D. T. Sandwell, Lithospheric flexure on Venus, *J. Geophys. Res., in press,* 1994.

Karate, S.1., M.S. Paterson, and J.D. Fitzgerald, Rheology of synthetic olivine aggregates: Influence of grain size and water, *J. Geophys. Res.,* 91, 8151-8176, 1986.

Kiefer, W. S., and B.H. Hager, A mantle plume model for the equatorial highlands of Venus, *J. Geophys. Res., 96, 20,947-20,966, 1991.*

Larson, R. L., Latest pulse of Earth: Evidence for a mid-Cretaceous superplume, Geology, *19*, 57-550, 1991.
Lindwall, D. A., A two-dimensional seismic investigation of crustal structure under the Hawaiian Islands near Oahu and Kauai, *J. Geophys. Res.*, 95', 12,107-12,122, 1988.
Liu, M., and C.G. Chase, Evolution of midplate hotspot swells: Numerical solutions, *J. Geophys. Res.*, 94, 5571-5584, 1989.
Mackwell, S. J., D. L. Kohlstedt, D. S. Scherber, and M. E. Zimmerman, High temperature deformation of diabase: Implications for tectonics on Venus, *Eos, Trans. Am. Geophys. Un., Full Meeting, 74, 378, 1993.*
Magna, M, H. A. Stone, and R.J. O'Connell, The interaction of plume heads with compositional discontinuities in the mantle, *J. Geophys. Res., 98, 19,979-19,990,)993.*
Monnereau, M., M. Rabinowicz, and E. Arquis, Mechanical erosion and reheating of the lithosphere: A numerical model for hotspot swells, *J. Geophys. Res.*, 96',809-823, 1993.
Nataf, H-C., and J. VanDecar, Seismological detection of a mantle plume? *Nature, 364, 115-120, 1993.*
Olson, P., and I. S. Nam, Formation of seafloor swells by mantle plumes, *J. Geophys. Res., 91*, 7181-7191, 1986.
Olsen, P., G. Schubert, and C. Anderson, Structure of axisymmetric mantle plumes, *J. Geophys. Res.*, 98, 6829-6844, 1993.
Parmentier, E. M., Thermal and compositional buoyancy in mantle plumes: implications for the structure of swells and temporal fluctuation of hot spot volcanism, *Eos Trans. Am. Geophys.* Un., 71, 1582, 1990.
Parmentier, E. M., and P. C. Hess, Chemical differentiation of a convecting planetary interior: Consequences for a one plate planet such as Venus, *Geophys. Res. Lett., 19*, 2015-2018, 1992.
Phillips, R. J., Convection-Driven tectonics on Venus, *J. Geophys. Res.*, 95, 1301-1316, 1990.
Philips, R. J., R.E. Grimm, and M.C. Malin, Hot-Spot evolution and the global tectonics of Venus, ***Science,*** 252, 651-658, 1991.
Phillips, R. J., R.R. Herrick, R.E. Grimm, R.F. Raubertas, I.C. Sarkar, R.E. Arvidson, and N. Izenberg, Impact crater distribution on Venus: Implications for planetary resurfacing, *J. Geophys. Res.*, 97, 15,923-15,948, 1992.
Phillips, R. J., Evaluation of Venus highland models, Icarus, in press, 1994.
Phillips, R.J., N.R. Isenberg, and J.S. Alexopoulus, Venus resurfacing history: Constraints from halo ejecta deposits, *Lunar Planet. Sci. Conf., 25, 1079-1080,* 1994.
Phipps Morgan, J., W.J. Morgan, and E. Price, Hotspot melting generates both hotspot volcanism and a hotspot swell?, *J. Geophys. Res.*, in press, 1994.
Ribe, N. M., and U.R. Christensen, Three-Dimensional modeling, of plume-lithosphere interaction, *J. Geophys. Res.*, 99, 669-682, 1994.
Richards, M. A., and B.H. Hager, Geoid anomalies in a dynamic Earth, *J. Geophys. Res.*, 89, 5987-6002,"1984.
Richards, M. A., B.H. Hager, and N.H. Sleep, Dynamically supported geoid highs over hotspots: Observations and theory, *J. Geophys. Res.*, 93, 7690-7708," 1988.
Robinson, E. M. , The topographic and gravitational expression of density anomalies due to melt extraction in the uppermost oceanic mantle. *Earth Planet. Sci. Lett.*, 90, 221-228, 1988.
Robinson, E. M., and B. Parsons, Effect of a shallow low-viscosity zone cm the formation of midplate swells, *J. Geophys. Res.*, 93, 3144-3156, 1988.
Sandwell, D. T., and G. Schubert, Flexural ridges, trenches, and outer rises around coronae on Venus. *J. Geophys. Res.*, 97, 16,069-16,084, 1992.
Schaber, G. G., R.G. Strom, H.J. Moore, L.A. Soderblom, R.L. Kirk, D.J. Chadwick, D.D. Dawson, L.R. Gaddis, J.M. Boyce, and J. Russell, Geology and distribution of

impact craters on Venus: What arc they telling us? *J. Geophys. Res.*, 97, 13,257-13,302, 1992.

Schaber, G. G., R.G. Strom, and D.J. Chadwick, Venus: Fractured craters revisited, and the evidence for minimal geologic activity over the past 300. my., Lunar Planet. Sci. Conf, 25, 119-1200, LPI, Houston, 1994.

Senske, D. A., G.G. Schaber, and E.R. Stofan, Regional topographic rises on Venus: Geology of Western Eistla Regio and comparison to Beta Regio and Atla Regio, *J. Geophys. Res.*, 97, 13,395-13,13,420, 1992.

Senske, D. A., R.S. Saunders, E.R. Stofan and Members of the Magellan Science Team, The global geology of Venus: Classification of landforms and geologic history, *Lunar* Planet. *Sci. Conf.* 2.5, 1245-1246, LPI, Houston, 1994.

Simons, M., B.H. Hager, S.C. Solomon, Global variations in geoid/topography admittance of Venus, Science, 264, 798-803, 1994.

Sleep, N. H., Hotspots and mantle plumes: Some phenomonology, *J. Geophys. Res.*, ***9.5,*** 6715-6736, 1990.

Smrekar, S., and R.J. Phillips, Venusian highlands: Geoid to topography ratios and their interpretation, *Earth Planet. Sci. Lett.*, *107, 582-597,* 1991.

Smrekar, S. E., Evidence for active hotspots on Venus from analysis of Magellan gravity data, *Icarus*, in press, 1994.

Solomon, S. C., and J. W. Head, Lithospheric flexure beneath the Freyja Montes foredeep, Venus: Constraints on lithospheric thermal gradients and heat flow. *Geophys. Res. Lett., 17, 1393-1396, 1990.*

Solomon, S. C., S. E. Smrekar, D. L. Bindschadler, R. E. Grimm, W. M. Kaula, G. E. McGill, R. J. Phillips, R. S. Saunders, G. Schubert, S. W. Squyres, and E. R. Stofan, Venus tectonics: An overview of Magellan Observations. *J. Geophys. Res.*, 97, 13.199-13.256. 1992.

Solomon, S. C., The geophysics of Venus, *Physics Today, July, 48-55, 1993.*

Stofan, E. R., V.L. Sharpton, G. Schubert, G. Baer, D.L. Bindschadler, D.M. Janes, S.W. Squyres, Global distribution and characteristics of coronae and related features on Venus: Implications for origin and relation to mantle processes, *J. Geophys. Res.*, 97, 13,347-13,378, 1992.

Stofan, E. R., D. Bindschadler, D. Senske, and S. E. Smrekar, Geologic and morphologic evidence for hotspot evolution on Venus, ***In preparation, 1994.***

Takahashi, E., and 1. Kushiro, Melting of a dry peridotite at high pressures and basalt magma genesis, *Am. Mineralogist, 68, 859-879,* 1983.

ten Brink, U. S., T.M. Brocher, Multichannel seismic evidence for a subcrustal intrusive complex under Oahu and a model for Hawaiian volcanism, *J. Geophys. Res.*, 92, 13,687-13,707, 1987.

Turcotte, D. L., An episodic hypothesis for Venusian tectonics, *J. Geophys. Res.*, 98, 17,061-17,068, 1993.

Waschbusch, P. J., and M.K. McNutt, Yellowstone: A continental midplate (hot spot) swell, *Geophys. Res. Lett., 21,] 703-1706,* 1 994

Watson, S., and D. McKenzie, Melt generation by plumes: A study of Hawaiian volcanism, *J. Petrol., 32, 501-537, 1991.*

Watts, A. B., U.S. ten Brink, P. Buhl, and T.M. Borcher, A multichannel seismic study of lithospheric structure across the Hawaiian-Emperor seamount chain, *Nature, 315,* 105-111, 1985.

White, R., Melt production rates in mantle plumes, *Phil. Trans. R. Sot. Lend. A,* 5'42, 137-153, 1993.

White, R., and D.P. McKenzie, Magmatism at rift zones: The generation of volcanic continental margins and flood basalts, *J. Geophys. Res.*, 94, 7685-7729, 19$9.

Wolfe, C. J., M.K. McNutt, and R.S. Dctrick, The Marquesas archipelagic apron: Seismic stratigraphy and implications for volcano growth, mass wasting, and crustal underplaying, *J. Geophys. Res.*, 99, 13,591-13,608, 1994.

Figure Captions

Figure 1. Plume-lithosphere interaction for the nominal case at (a) 43 my., (h) 109 my., (c) 169 my., and (d) 259 my. after the start of the calculation. Color indicates temperature; red is -1 500°C, yellow-green is -1300°C, green is -1 100"C, and dark blue is ~500°C. Black lines arc contours of depletion for values of 1 and 10% depletion. The initial layer of depleted mantle, assumed to be 20% depleted, extends to a depth of 150 km. The base of the thermal lithosphere, as defined by the 11 00°C contour, is at a depth of 100 km. Black arrows mark the flow pattern, with an arrow shown at every other finite element node. Figure 1a shows the entire 2400 km x 2400 km computational domain, before the plume head interacts with the lithosphere. Figures 1b-d show only the upper 600 km near the plume head. These figures illustrate the plume head spreading out in early, intermediate and late stages of plume evolution. A significant melt volume is not produced until approximately 50 my. after the plume reaches the lithosphere (Figure 1c). Thinning of the thermal and chemical boundary layers is evident in Figures 1c and 1d.

"Figure 2. The topography and geoid for the nominal case at 11 non-uniformly spaced time steps cm-responding to times between O and 350 my. after the start of the calculation. The dashed lines indicate the four time steps shown in Figure 1. The topography skirts out as a relatively narrow rise, broadens as the plume head spreads out at the base of the lithosphere and eventually dies out. The geoid is calculated at an altitude of 3(K) km for comparison to data for Venus. The contribution to the geoid from the density anomaly due to the topography is shown separately from that due to thermal and chemical density anomalies. The total geoid is the sum of the two components.

Figure 3. Predicted buoyancy flux, GTR, swell and melt volumes, and maximum topography for the nominal case. Buoyancy flux calculation are based on swell volume, chemical density changes relative to the undisturbed, initial model, and on excess plume temperature. The cumulative swell and melt volumes are plotted on a log scale in the lower left. The GTR and maximum topography arc shown in the upper and lower right, respectively.

Figure 4. Maximum topography, GTR, and cumulative melt volume as a function of time for cases with thermal lithospheric thicknesses of 50, 1(M), and 150 km, with no layer of depleted mantle. The plume is turned off after 150 m .y.

Figure 5. Maximum topography, GTR, and cumulative melt volume as a function of time for cases with a 100 km thick thermal lithosphere and depleted layer thicknesses of 0, 150, 200, and 250 km. The plume is turned off after 150 my.

Figure 6. Same as Figure 5, except that in these models the viscosity is assumed to increase by a factor of ten for values of depletion in excess of 2%.

Figure 7. Maximum topography, GTR, and cumulative melt volume as a function of time for cases with initial maximum plume temperatures of 350, 450, and 550°C greater than the mantle temperature of 1300°C. Near surface maximum temperature differences between the plume and mantle are approximately 180, 200, and 220°C. The plume is turned off after 150 my.

Figure 8. Maximum topography, GTR, and cumulative melt volume as a function of time for cases in which the depleted layer, D, varies from () to 250 km in thickness and the plume is active for 250 my. See Figure 5 for comparison to cases in which the plume is turned off after 150 my.

Figure 9. The cumulative melt column height for pressure-release melting as a function of distance from the axis for a case in which the mantle temperature is 1300°C, the initial plume temperature is 1850°C, and the final cumulative melt volume is -105 km^3 (see Figure 7 for GTR, topography and melting history of this model).

Figure 10. Effects of a volcanic edifice cm GTR, using the same model as in Figure 9 as an example. The volume of pressure-release melting is assumed to form a volcano with a slope of ().5°. The final size of the volcano is 2.5 km in height and 500 km in diameter, and is typical of large edifices at venusian hotspots. If the volcano is crustally compensated, the GTR is slightly decreased. An uncompensated (or flexurally compensated) volcano can make a contribution of up to 5 m/km to the GTR.

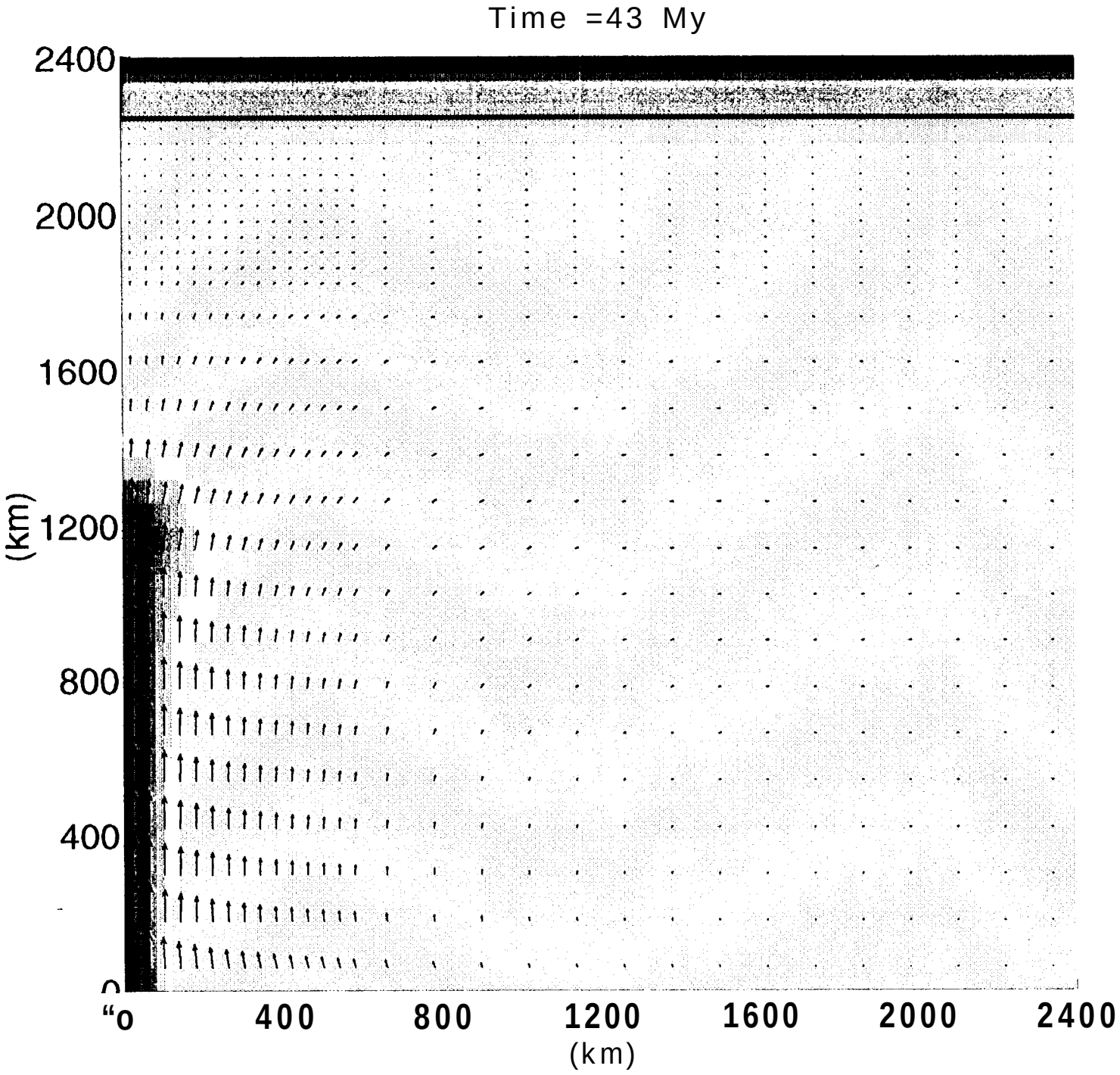
Time =43 My
2400
2000
1600
1200
800
400
0
(km)
"o
400
800
1200
1600
2000
2400
(km)

Figure la.

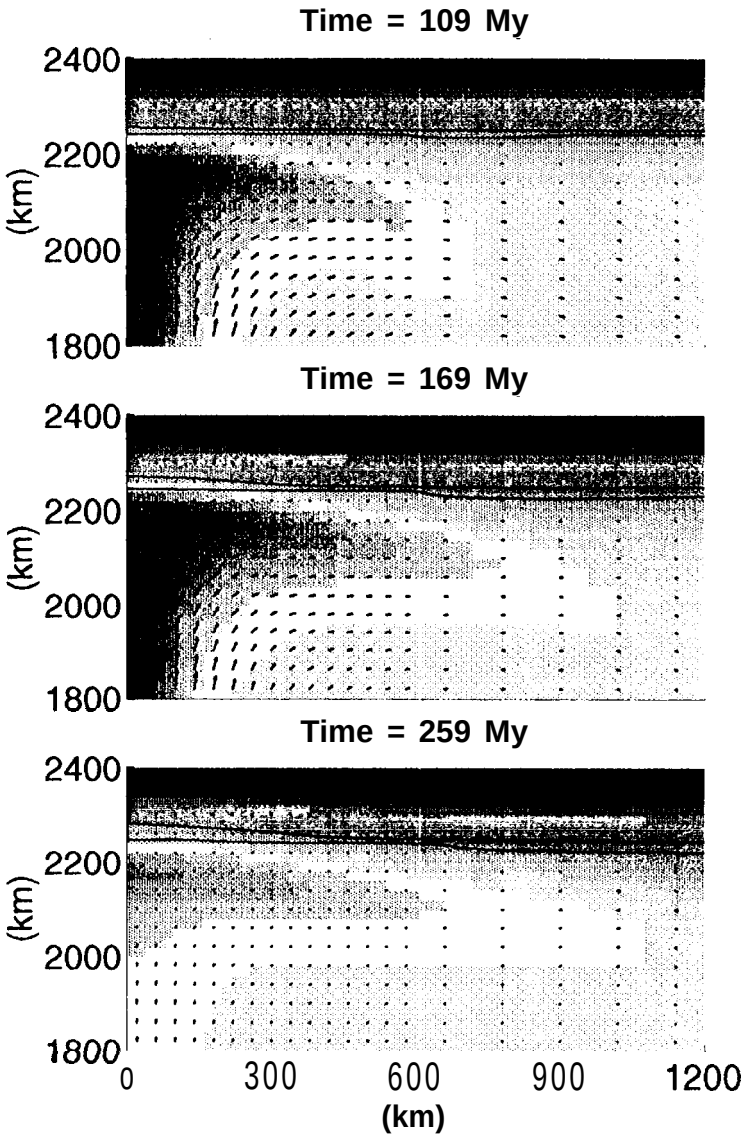
Time = 109 My
Time = 169 My
Time = 259 My
2400
2200
2000
1800
(km)
0
300
600
900
1200
(km)

Figure lb, c,d.

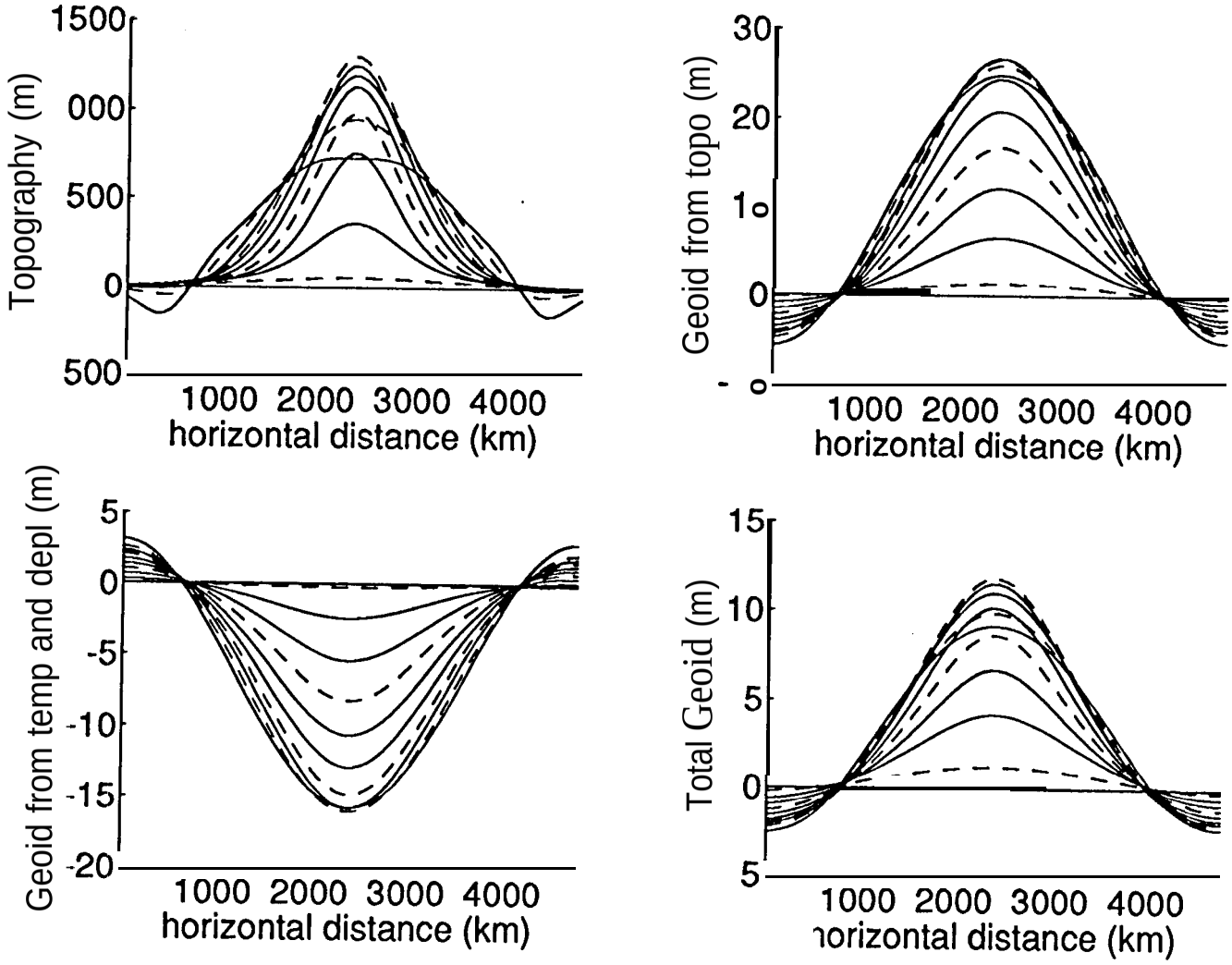
Topography (m)
1500
000
500
0
500
1000 2000 3000 4000
horizontal distance (km)
Geoid from topo (m)
30
20
1o
0
-
o
1000 2000 3000 4000
horizontal distance (km)
Geoid from temp and depl (m)
5
0
-5
-10
-15
-20
1000 2000 3000 4000
horizontal distance (km)
Total Geoid (m)
15
10
5
0
5
1000 2000 3000 4000
horizontal distance (km)

Figure 2.

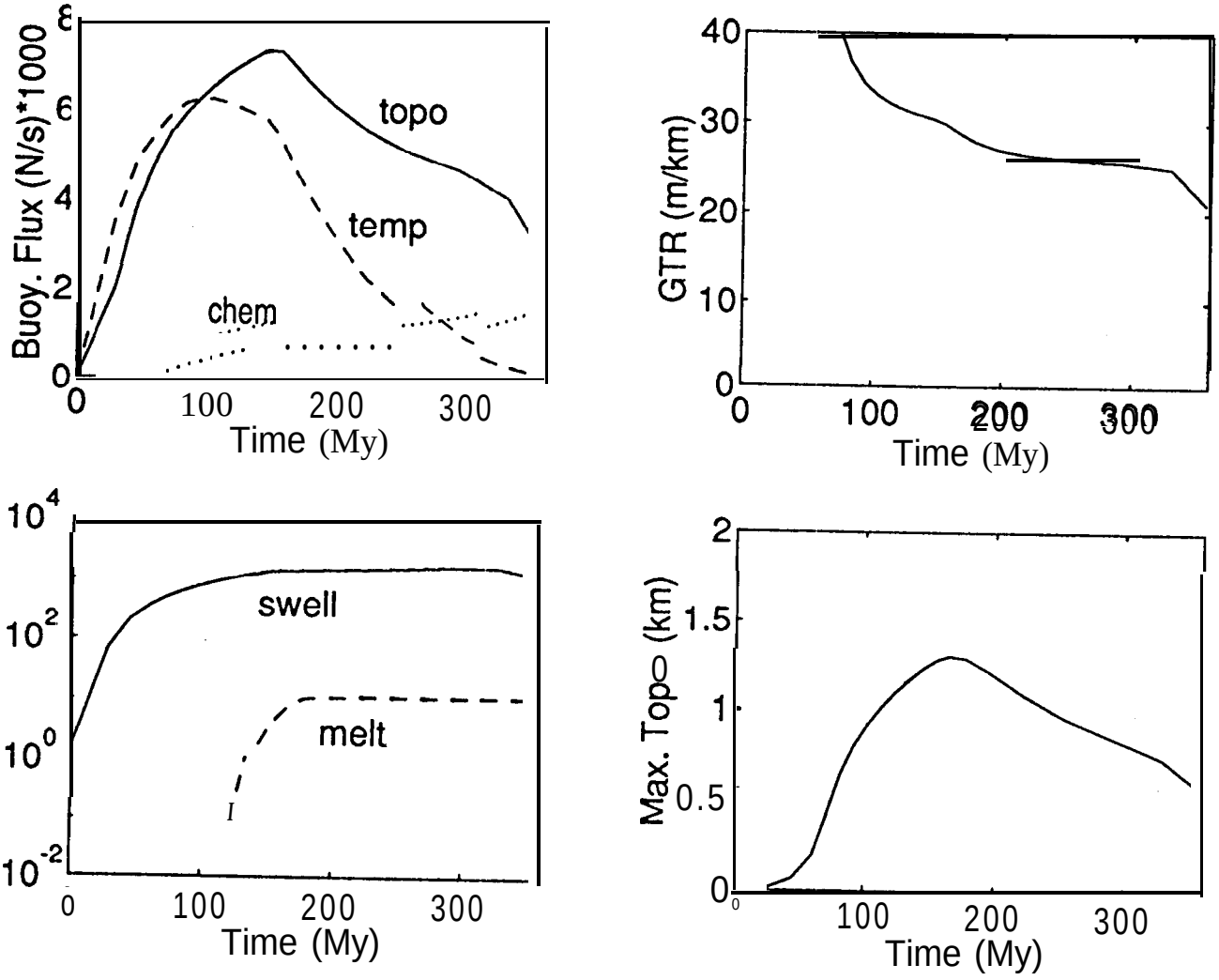
Buoy. Flux (N/s)*1000
topo
temp
chem
Time (My)
GTR (m/km)
Time (My)
Volume (km3)*1000
swell
melt
Time (My)
Max. Topo (km)
Time (My)

Figure 3

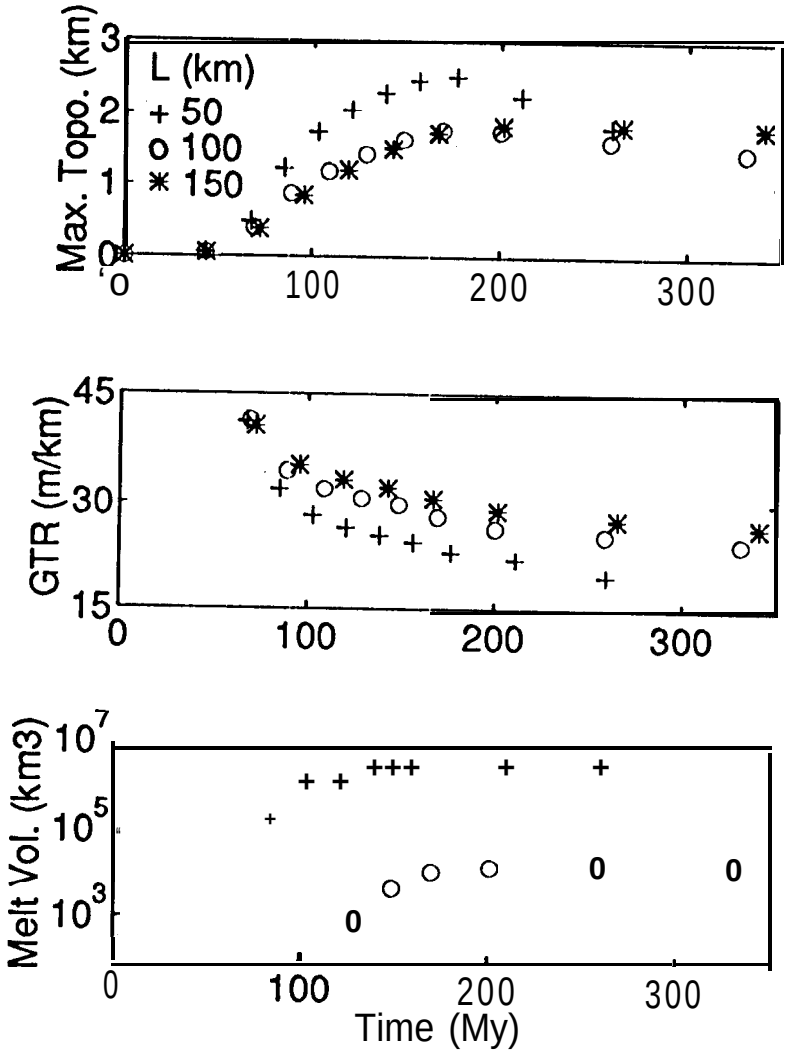

Figure 4.

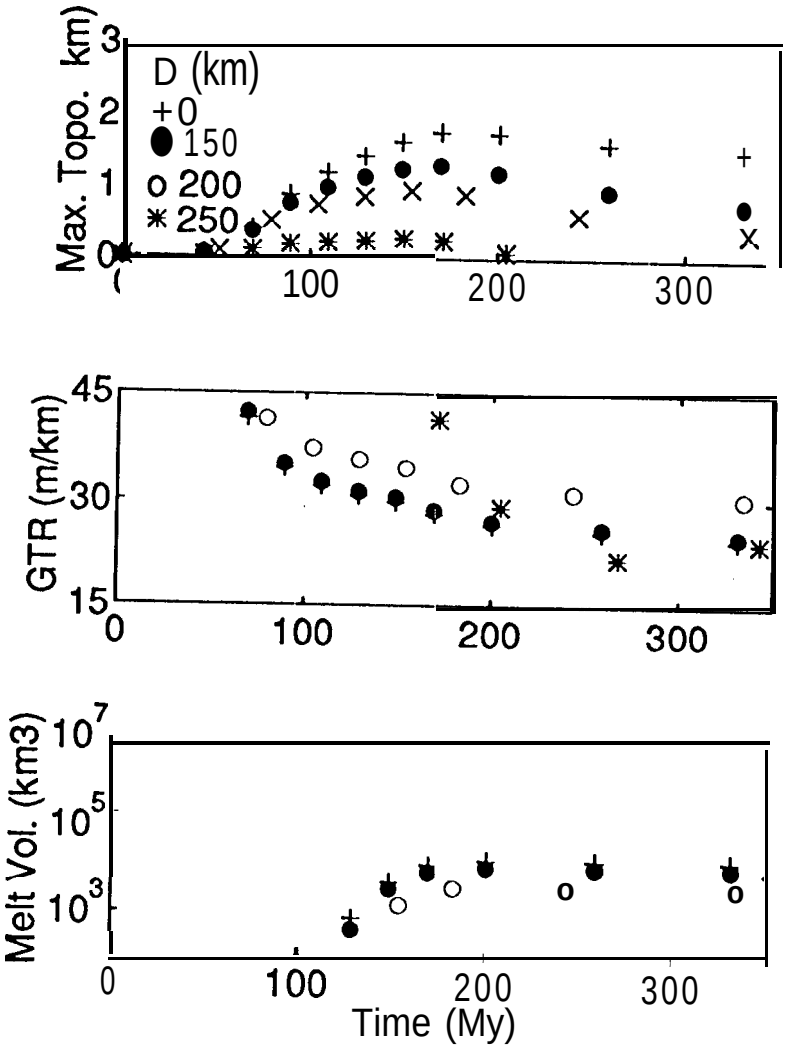
Max. Topo. km)
3
2
1
0
D (km)
+0
150
o 200
* 250
100
200
300
GTR (m/km)
45
30
15
0
100
200
300
Melt Vol. (km3)
10^7
10^5
10^3
0
100
200
300
Time (My)

Figure 5.

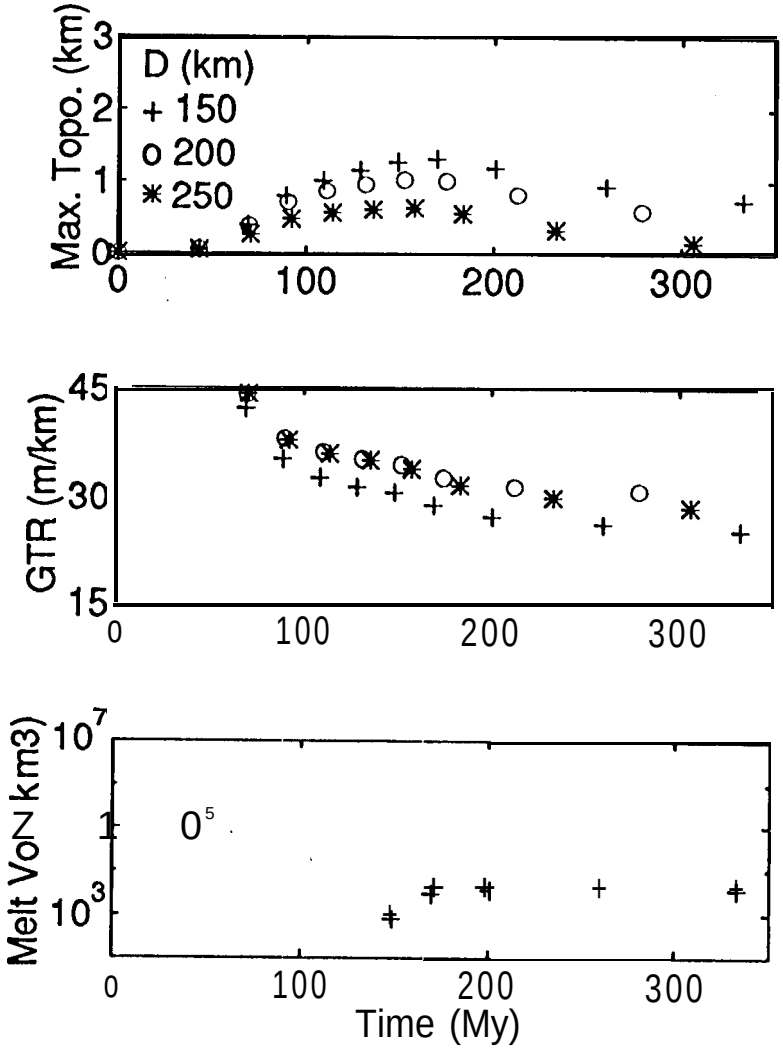

Figure 6.

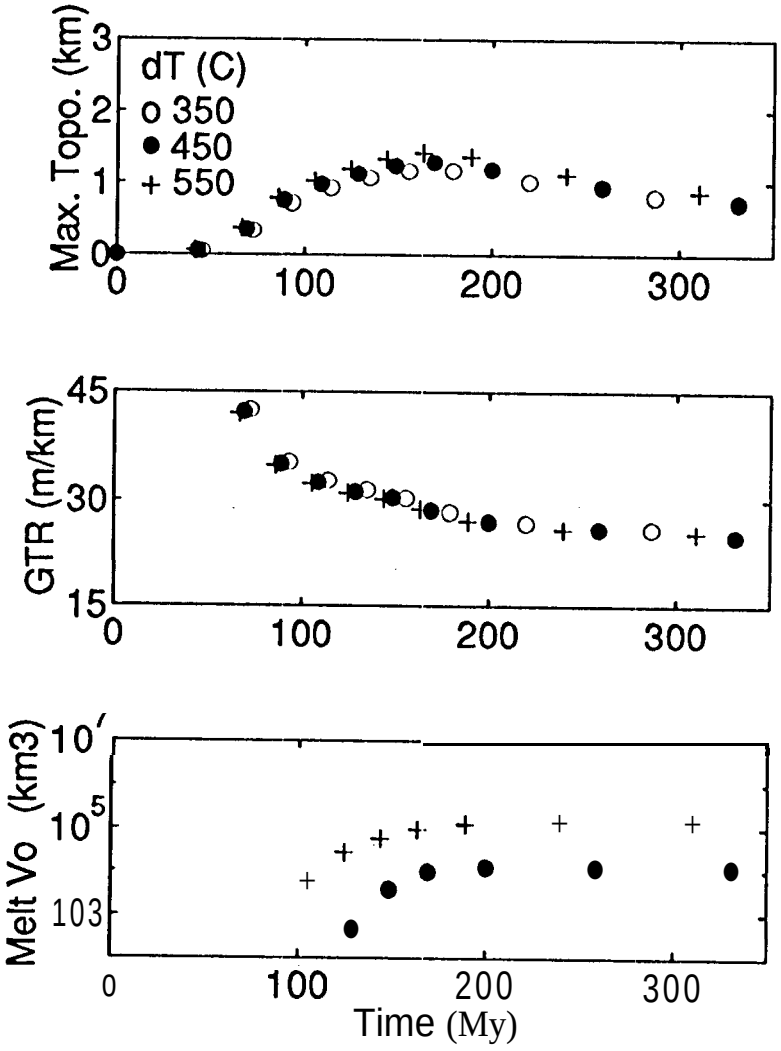

Figure 7.

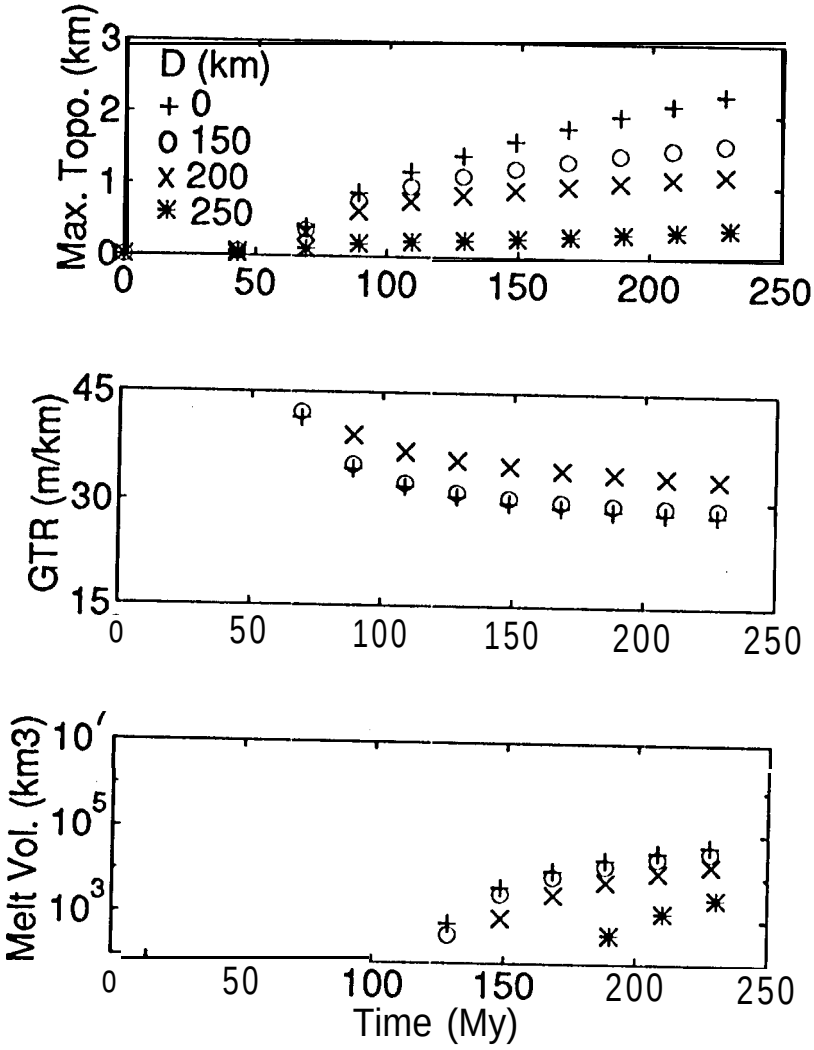

Figure 8.

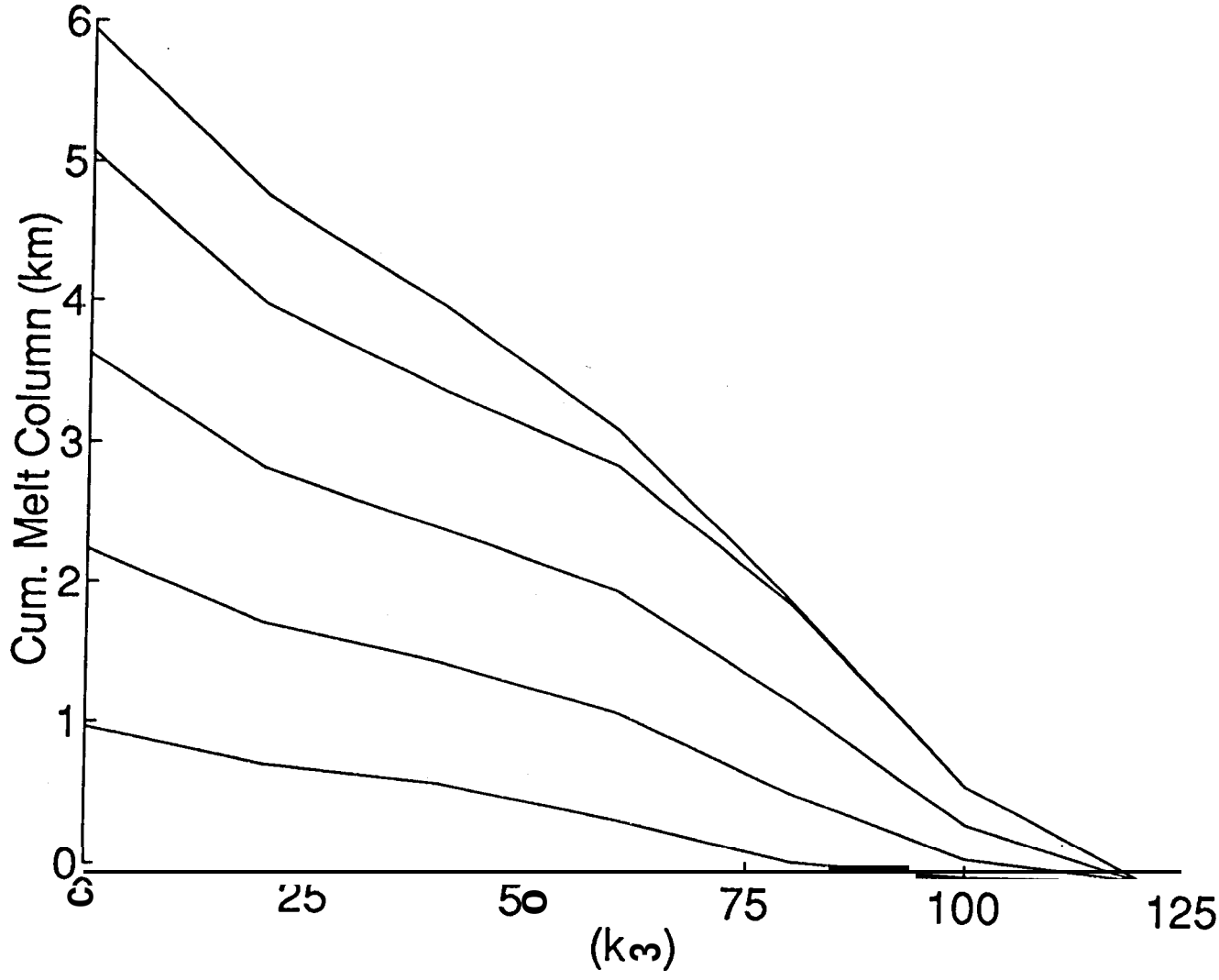
Cum. Melt Column (km)
6
5
4
3
2
1
0
0
25
50
75
100
125
(km)

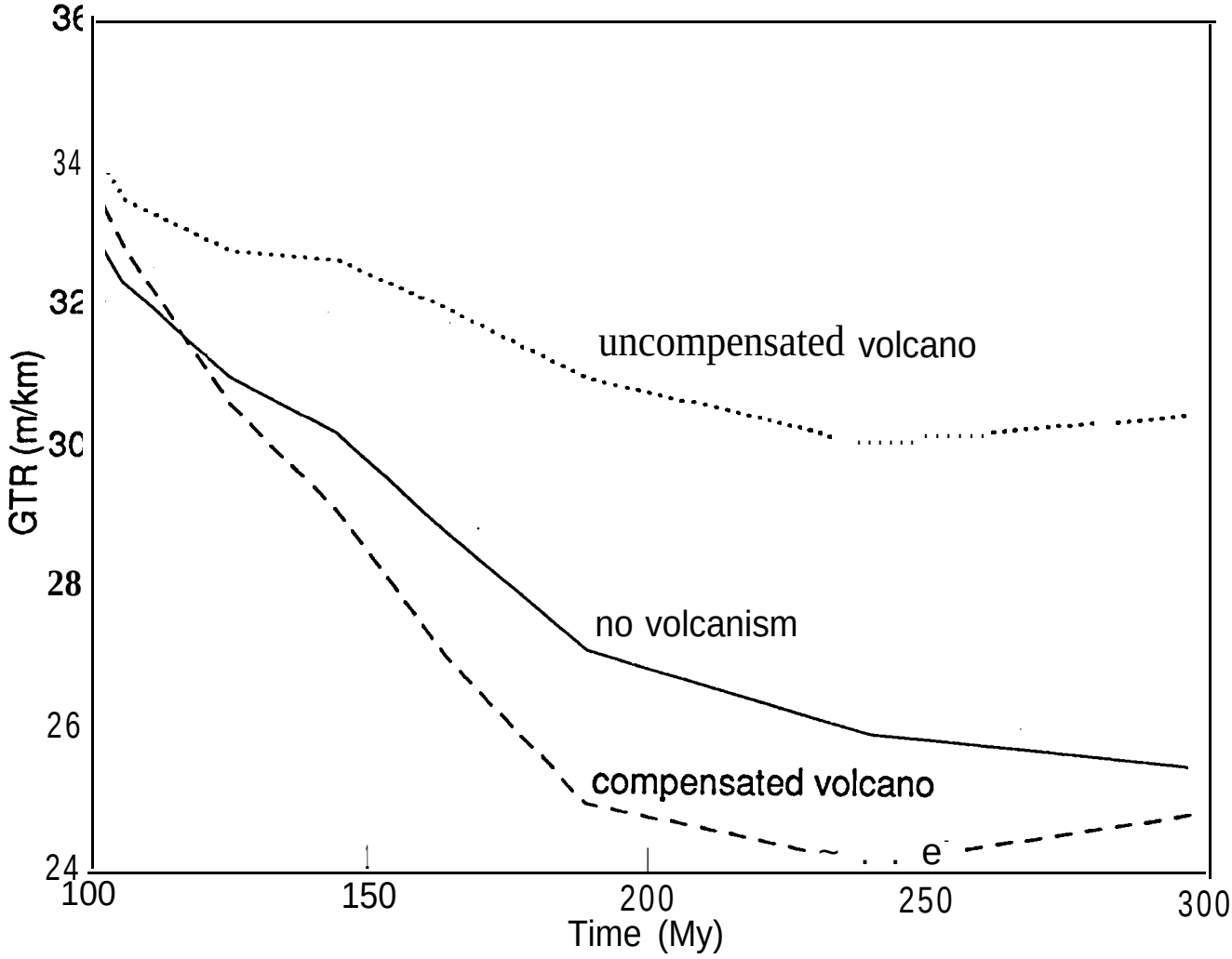
36
34
32
30
28
26
24
GTR (m/km)
uncompensated volcano
no volcanism
compensated volcano
e
100
150
200
250
300
Time (My)

Figure 10.